

# Guidelines for the Echocardiographic Assessment of the Right Heart in Adults: A Report from the American Society of Echocardiography

Endorsed by the European Association of Echocardiography, a registered branch of the European Society of Cardiology, and the Canadian Society of Echocardiography

Lawrence G. Rudski, MD, FASE, Chair, Wyman W. Lai, MD, MPH, FASE, Jonathan Afilalo, MD, Msc, Lanqi Hua, RDCS, FASE, Mark D. Handschumacher, BSc, Krishnaswamy Chandrasekaran, MD, FASE, Scott D. Solomon, MD, Eric K. Louie, MD, and Nelson B. Schiller, MD, *Montreal, Quebec, Canada; New York, New York; Boston, Massachusetts; Phoenix, Arizona; London, United Kingdom; San Francisco, California*

(J Am Soc Echocardiogr 2010;23:685-713.)

**Keywords:** Right ventricle, Echocardiography, Right atrium, Guidelines

### Accreditation Statement:

The American Society of Echocardiography is accredited by the Accreditation Council for Continuing Medical Education to provide continuing medical education for physicians. The American Society of Echocardiography designates this educational activity for a maximum of 1.0 AMA PRA Category 1 Credits™. Physicians should only claim credit commensurate with the extent of their participation in the activity.

ARDMS and CCI recognize ASE's certificates and have agreed to honor the credit hours toward their registry requirements for sonographers.

The American Society of Echocardiography is committed to ensuring that its educational mission and all sponsored educational programs are not influenced by the special interests of any corporation or individual, and its mandate is to retain only those authors whose financial interests can be effectively resolved to maintain the goals and educational integrity of the activity. While a monetary or professional affiliation with a corporation does not necessarily influence an author's presentation, the Essential Areas and policies of the ACCME require that any relationships that could possibly conflict with the educational value of the activity be resolved prior to publication and disclosed to the audience. Disclosures of faculty and commercial support relationships, if any, have been indicated.

### Target Audience:

This activity is designed for all cardiovascular physicians and cardiac sonographers with a primary interest and knowledge base in the field of echocardiography; in addition, residents, researchers, clinicians, intensivists, and other medical professionals with a specific interest in cardiac ultrasound will find this activity beneficial.

### Objectives:

Upon completing the reading of this article, the participants will better be able to:

1. Describe the conventional two-dimensional acoustic windows required for optimal evaluation of the right heart.
2. Describe the echocardiographic parameters required in routine and directed echocardiographic studies, and the views to obtain these parameters for assessing right ventricle (RV) size and function.
3. Identify the advantages and disadvantages of each measure or technique as supported by the available literature.
4. Recognize which right-sided measures should be included in the standard echocardiographic report.
5. Explain the clinical and prognostic significance of right ventricular assessment.

### Author Disclosure:

The authors of this article reported no actual or potential conflicts of interest in relation to this activity.

The ASE staff and ASE ACCME/CME reviewers who were involved in the planning and development of this activity reported no actual or potential conflicts of interest: Chelsea Flowers; Rebecca T. Hahn, MD, FASE; Cathy Kerr; Priscilla P. Peters, BA, RDCS, FASE; Rhonda Price; and Cheryl Williams.

The following members of the ASE Guidelines and Standards Committee, JASE Editorial staff and ASE Board of Directors reported no actual or potential conflicts of interest in relation to this activity: Deborah A. Agler, RCT, RDCS, FASE; J. Todd Belcik, BS, RDCS, FASE; Renee L. Bess, BS, RDCS, RVT, FASE; Farooq A. Chaudhry, MD, FASE; Robert T. Eberhardt, MD; Benjamin W. Eidem, MD, FASE; Gregory J. Ensing, MD, FASE; Tal Geva, MD, FASE; Kathryn E. Glas, MD, FASE; Sandra Hagen-Ansert, RDCS, RDMS, MS, FASE; Rebecca T. Hahn, MD, FASE; Jeannie Heirs, RDCS; Shunichi Homma, MD; Sanjiv Kaul, MD, FASE; Smadar Kort, MD, FASE; Peg Knoll, RDCS, FASE; Wyman Lai, MD, MPH, FASE; Roberto M. Lang, MD, FASE; Steven Lavine, MD; Steven J. Lester, MD, FASE; Renee Margossian, MD; Victor Mor-Avi, PhD, FASE; Sherif Nagueh, MD, FASE; Alan S. Pearlman, MD, FASE; Patricia A. Pellikka, MD, FASE; Miguel Quiñones, MD, FASE; Brad Roberts, RCS, RDCS; Beverly Smulevitz, BS, RDCS, RVS; Kirk T. Spencer, MD, FASE; J. Geoffrey Stevenson, MD, FASE; Wadea Tarhuni, MD, FASE; James D. Thomas, MD; Neil J. Weissman, MD, FASE; Timothy Woods, MD; and William A. Zoghbi, MD, FASE.

The following members of the ASE Guidelines and Standards Committee, JASE Editorial staff and ASE Board of Directors reported a relationship with one or more commercial interests. According to ACCME policy, the ASE implemented mechanisms to resolve all conflicts of interest prior to the planning and implementation of this activity. Theodore Abraham, MD, FASE receives honoraria and research grant support from GE Healthcare. Patrick D. Coon, RDCS, FASE is on the speaker's bureau for Philips. Victor G. Davila-Roman, MD, FASE is a consultant for St. Jude Medical, AGA Medical, Medtronic, Boston Scientific Corporation, and Sadra Medical. Elyse Foster, MD receives grant support from Abbott Vascular Structural Heart, EBR Systems, Inc., and Boston Scientific Corporation. Julius M. Gardin, MD, FASE is a consultant/advisor to Arena Pharmaceuticals. Jeffrey C. Hill, BS, RDCS, FASE receives grant/research support from Toshiba America Medical Systems and Philips; is a consultant to Medtronic; and is on the speaker's bureau for Philips. Martin G. Keane, MD, FASE is a consultant/advisor to Pfizer, Inc. and Otsuka Pharmaceuticals. Gilead I. Lancaster, MD, FASE owns stock in, and is a consultant/advisor to, Cardiogal. Jonathan R. Linder, MD, FASE is a consultant/advisor to VisualSonics. Carol C. Mitchell, PhD, RDMS, RDCS, RVT, RT(R), FASE is a speaker and consultant for GE Healthcare. Marti McCulloch, MBA, BS, RDCS, FASE is a speaker for Lantheus and advisor/consultant for Siemens. Tasneem Z. Naqvi, MD, FASE is a consultant/advisor to Edwards Lifesciences and St. Jude Medical, and receives grant support from Medtronic and Actor Medical. Kofo O. Ogunyankin, MD, FASE is on the speaker's bureau for Lantheus. Vera Rigolin, MD, FASE is on the speaker's bureau for Edwards Lifesciences and St. Jude Medical and owns stock in Abbott Labs; Hospira; Johnson and Johnson; and Medtronic. Lawrence G. Rudski, MD receives grant support from Genzyme. Stephen G. Sawada, MD owns stock in GE Healthcare. Alan D. Waggoner, MHS, RDCS is a consultant/advisor for Boston Scientific Corporation and St. Jude Medical, Inc.

Estimated Time to Complete This Activity: 1.0 hour

From the Jewish General Hospital, McGill University, Montreal, Quebec, Canada (L.G.R., J.A.); Morgan Stanley Children's Hospital of New York Presbyterian, New York, New York (W.W.L.); Massachusetts General Hospital, Boston, Massachusetts (M.D.H., L.H.); Mayo Clinic, Phoenix, Arizona (K.C.); Brigham and Women's Hospital, Harvard Medical School, Boston, Massachusetts (S.D.S.); Sg2, LLC, London, United Kingdom (E.K.L.); and the University of California, San Francisco, San Francisco, California (N.B.S.).

Reprint requests: American Society of Echocardiography, 2100 Gateway Centre Boulevard, Suite 310, Morrisville, NC 27560 (E-mail: [ase@asecho.org](mailto:ase@asecho.org)).

0894-7317/\$36.00

Copyright 2010 by the American Society of Echocardiography.

doi:10.1016/j.echo.2010.05.010

**TABLE OF CONTENTS**

Executive Summary	686
Overview	688
Methodology in the Establishment of Reference Value and Ranges	688
Acoustic Windows and Echocardiographic Views of the Right Heart	690
Nomenclature of Right Heart Segments and Coronary Supply	690
Conventional Two-Dimensional Assessment of the Right Heart	690
A. Right Atrium	690
RA Pressure	691
B. Right Ventricle	692
RV Wall Thickness	692
RV Linear Dimensions	693
C. RVOT	694
Fractional Area Change and Volumetric Assessment of the Right Ventricle	696
A. RV Area and FAC	696
B. Two-Dimensional Volume and EF Estimation	696
C. Three-Dimensional Volume Estimation	697
The Right Ventricle and Interventricular Septal Morphology	697
A. Differential Timing of Geometric Distortion in RV Pressure and Volume Overload States	698
Hemodynamic Assessment of the Right Ventricle and Pulmonary Circulation	698
A. Systolic Pulmonary Artery Pressure	698
B. PA Diastolic Pressure	699
C. Mean PA Pressure	699
D. Pulmonary Vascular Resistance	699
E. Measurement of PA Pressure During Exercise	699
Nonvolumetric Assessment of Right Ventricular Function	700
A. Global Assessment of RV Systolic Function	700
RV dP/dt	700
RIMP	700
B. Regional Assessment of RV Systolic Function	701
TAPSE or Tricuspid Annular Motion (TAM)	701
Doppler Tissue Imaging	702
Myocardial Acceleration During Isovolumic Contraction	703
Regional RV Strain and Strain Rate	704
Two-Dimensional Strain	705
Summary of Recommendations for the Assessment of Right Ventricular Systolic Function	705
Right Ventricular Diastolic Function	705
A. RV Diastolic Dysfunction	705
B. Measurement of RV Diastolic Function	705
C. Effects of Age, Respiration, Heart Rate, and Loading Conditions	706
D. Clinical Relevance	706
Clinical and Prognostic Significance of Right Ventricular Assessment	706
References	708

**EXECUTIVE SUMMARY**

The right ventricle plays an important role in the morbidity and mortality of patients presenting with signs and symptoms of cardiopulmonary disease. However, the systematic assessment of right heart function is not uniformly carried out. This is due partly to the enormous attention given to the evaluation of the left heart, a lack of familiarity with ultrasound techniques that can be used in imaging the right

heart, and a paucity of ultrasound studies providing normal reference values of right heart size and function.

**In all studies, the sonographer and physician should examine the right heart using multiple acoustic windows, and the report should represent an assessment based on qualitative and quantitative parameters. The parameters to be performed and reported should include a measure of right ventricular (RV) size, right atrial (RA) size, RV systolic function (at least one of the following: fractional area change [FAC],  $S'$ , and tricuspid annular plane systolic excursion [TAPSE]; with or without RV index of myocardial performance [RIMP]), and systolic pulmonary artery (PA) pressure (SPAP) with estimate of RA pressure on the basis of inferior vena cava (IVC) size and collapse. In many conditions, additional measures such as PA diastolic pressure (PADP) and an assessment of RV diastolic function are indicated. The reference values for these recommended measurements are displayed in Table 1. These reference values are based on values obtained from normal individuals without any histories of heart disease and exclude those with histories of congenital heart disease. Many of the recommended values differ from those published in the previous recommendations for chamber quantification of the American Society of Echocardiography (ASE). The current values are based on larger populations or pooled values from several studies, while several previous normal values were based on a single study. It is important for the interpreting physician to recognize that the values proposed are not indexed to body surface area or height. As a result, it is possible that patients at either extreme may be misclassified as having values outside the reference ranges. The available data are insufficient for the classification of the abnormal categories into mild, moderate, and severe. Interpreters should therefore use their judgment in determining the extent of abnormality observed for any given parameter. As in all studies, it is therefore critical that all information obtained from the echocardiographic examination be considered in the final interpretation.**

**Essential Imaging Windows and Views**

Apical 4-chamber, modified apical 4-chamber, left parasternal long-axis (PLAX) and parasternal short-axis (PSAX), left parasternal RV inflow, and subcostal views provide images for the comprehensive assessment of RV systolic and diastolic function and RV systolic pressure (RVSP).

**Right Heart Dimensions.** **RV DIMENSION.** RV dimension is best estimated at end-diastole from a right ventricle–focused apical 4-chamber view. Care should be taken to obtain the image demonstrating the maximum diameter of the right ventricle without foreshortening (Figure 6). This can be accomplished by making sure that the crux and apex of the heart are in view (Figure 7). **Diameter > 42 mm at the base and > 35 mm at the mid level indicates RV dilatation. Similarly, longitudinal dimension > 86 mm indicates RV enlargement.**

**RA DIMENSION.** The apical 4-chamber view allows estimation of the RA dimensions (Figure 3). **RA area > 18 cm<sup>2</sup>, RA length (referred to as the major dimension) > 53 mm, and RA diameter (otherwise known as the minor dimension) > 44 mm indicate at end-diastole RA enlargement.**

## Abbreviations

<b>ASE</b> = American Society of Echocardiography
<b>AT</b> = Acceleration time
<b>EF</b> = Ejection fraction
<b>ET</b> = Ejection time
<b>FAC</b> = Fractional area change
<b>IVA</b> = Isovolumic acceleration
<b>IVC</b> = Inferior vena cava
<b>IVCT</b> = Isovolumic contraction time
<b>IVRT</b> = Isovolumic relaxation time
<b>MPI</b> = Myocardial performance index
<b>MRI</b> = Magnetic resonance imaging
<b>LV</b> = Left ventricle
<b>PA</b> = Pulmonary artery
<b>PADP</b> = Pulmonary artery diastolic pressure
<b>PH</b> = Pulmonary hypertension
<b>PLAX</b> = Parasternal long-axis
<b>PSAX</b> = Parasternal short-axis
<b>PVR</b> = Pulmonary vascular resistance
<b>RA</b> = Right atrium
<b>RIMP</b> = Right ventricular index of myocardial performance
<b>RV</b> = Right ventricle
<b>RVH</b> = Right ventricular hypertrophy
<b>RVOT</b> = Right ventricular outflow tract
<b>RVSP</b> = Right ventricular systolic pressure
<b>SD</b> = Standard deviation
<b>SPAP</b> = Systolic pulmonary artery pressure
<b>TAM</b> = Tricuspid annular motion
<b>TAPSE</b> = Tricuspid annular plane systolic excursion
<b>3D</b> = Three-dimensional
<b>TR</b> = Tricuspid regurgitation
<b>2D</b> = Two-dimensional

**RV OUTFLOW TRACT (RVOT) DIMENSION.** The left PSAX view demonstrating RVOT at the level of the pulmonic valve yields the “distal diameter” (Figure 8C), while the left PLAX view allows for the measurement of the proximal portion of the RVOT, also referred to as “proximal diameter” (Figure 8A). **Diameter > 27 mm at end-diastole at the level of pulmonary valve insertion (“distal diameter”) indicates RVOT dilatation.**

**RV WALL THICKNESS.** RV wall thickness is measured in diastole, preferably from the subcostal view, using either M-mode or two-dimensional (2D) imaging (Figure 5). Alternatively, the left parasternal view is also used for measuring RV wall thickness. **Thickness > 5 mm indicates RV hypertrophy (RVH) and may suggest RV pressure overload in the absence of other pathologies.**

**Table 1** Summary of reference limits for recommended measures of right heart structure and function

Variable	Unit	Abnormal	Illustration
<b>Chamber dimensions</b>			
RV basal diameter	cm	>4.2	Figure 7
RV subcostal wall thickness	cm	>0.5	Figure 5
RVOT PSAX distal diameter	cm	>2.7	Figure 8
RVOT PLAX proximal diameter	cm	>3.3	Figure 8
RA major dimension	cm	>5.3	Figure 3
RA minor dimension	cm	>4.4	Figure 3
RA end-systolic area	cm <sup>2</sup>	>18	Figure 3
<b>Systolic function</b>			
TAPSE	cm	<1.6	Figure 17
Pulsed Doppler peak velocity at the annulus	cm/s	<10	Figure 16
Pulsed Doppler MPI	—	>0.40	Figure 16
Tissue Doppler MPI	—	>0.55	Figures 16 and 18
FAC (%)	%	<35	Figure 9
<b>Diastolic function</b>			
E/A ratio	—	<0.8 or >2.1	
E/E' ratio	—	>6	
Deceleration time (ms)	ms	<120	

FAC, Fractional area change; MPI, myocardial performance index; PLAX, parasternal long-axis; PSAX, parasternal short-axis; RA, right atrium; RV, right ventricle; RVD, right ventricular diameter; RVOT, right ventricular outflow tract; TAPSE, tricuspid annular plane systolic excursion.

**IVC DIMENSION.** The subcostal view permits imaging and measurement of the IVC and also assesses inspiratory collapsibility. IVC diameter should be measured just proximal to the entrance of hepatic veins (Figure 4). **For simplicity and uniformity of reporting, specific values of RA pressure, rather than ranges, should be used in the determination of SPAP. IVC diameter ≤ 2.1 cm that collapses >50% with a sniff suggests normal RA pressure of 3 mm Hg (range, 0-5 mm Hg), whereas IVC diameter > 2.1 cm that collapses < 50% with a sniff suggests high RA pressure of 15 mm Hg (range, 10-20 mm Hg). In scenarios in which IVC diameter and collapse do not fit this paradigm, an intermediate value of 8 mm Hg (range, 5-10 mm Hg) may be used or, preferably, other indices of RA pressure should be integrated to downgrade or upgrade to the normal or high values of RA pressure.** It should be noted that in normal young athletes, the IVC may be dilated in the presence of normal pressure. In addition, the IVC is commonly dilated and may not collapse in patients on ventilators, so it should not be used in such cases to estimate RA pressure.

**RV Systolic Function.** RV systolic function has been evaluated using several parameters, namely, RIMP, TAPSE, 2D RV FAC, 2D RV ejection fraction (EF), three-dimensional (3D) RV EF, tissue Doppler-derived tricuspid lateral annular systolic velocity (S'), and longitudinal strain and strain rate. Among them, more studies have demonstrated the clinical utility and value of RIMP, TAPSE, 2D FAC, and S' of the tricuspid annulus. Although 3D RV EF seems to be more reliable with fewer reproducibility errors, there are insufficient data demonstrating its clinical value at present.

**RIMP** provides an index of global RV function. **RIMP > 0.40 by pulsed Doppler and > 0.55 by tissue Doppler** indicates RV dysfunction. By measuring the isovolumic contraction time (IVCT), isovolumic relaxation time (IVRT), and ejection time (ET) indices from the pulsed tissue Doppler velocity of the lateral tricuspid annulus, one avoids errors related to variability in the heart rate. RIMP can be falsely low in conditions associated with elevated RA pressures, which will decrease the IVRT.

**TAPSE** is easily obtainable and is a measure of RV longitudinal function. **TAPSE < 16 mm** indicates RV systolic dysfunction. It is measured from the tricuspid lateral annulus. Although it measures longitudinal function, it has shown good correlation with techniques estimating RV global systolic function, such as radionuclide-derived RV EF, 2D RV FAC, and 2D RV EF.

**Two-dimensional FAC** (as a percentage) provides an estimate of RV systolic function. **Two-dimensional FAC < 35%** indicates RV systolic dysfunction. It is important to make sure that the entire right ventricle is in the view, including the apex and the lateral wall in both systole and diastole. Care must be taken to exclude trabeculations while tracing the RV area.

**S'** is easy to measure, reliable and reproducible. **S' velocity < 10 cm/s** indicates RV systolic dysfunction. S' velocity has been shown to correlate well with other measures of global RV systolic function. It is important to keep the basal segment and the annulus aligned with the Doppler cursor to avoid errors.

**RV Diastolic Dysfunction.** Assessment of RV diastolic function is carried out by pulsed Doppler of the tricuspid inflow, tissue Doppler of the lateral tricuspid annulus, pulsed Doppler of the hepatic vein, and measurements of IVC size and collapsibility. Various parameters with their upper and lower reference ranges are shown in Table 1. Among them, the E/A ratio, deceleration time, the E/e' ratio, and RA size are recommended. Note that these parameters should be obtained at end-expiration during quiet breathing or as an average of  $\geq 5$  consecutive beats and that they may not be valid in the presence of significant tricuspid regurgitation (TR).

**GRADING OF RV DIASTOLIC DYSFUNCTION.** A tricuspid **E/A ratio < 0.8** suggests impaired relaxation, a tricuspid **E/A ratio of 0.8 to 2.1 with an E/e' ratio > 6** or diastolic flow predominance in the hepatic veins suggests pseudonormal filling, and a tricuspid **E/A ratio > 2.1 with deceleration time < 120 ms** suggests restrictive filling.

**Pulmonary Systolic Pressure/RVSP.** TR velocity reliably permits estimation of RVSP with the addition of RA pressure, assuming no significant RVOT obstruction. It is recommended to use the RA pressure estimated from IVC and its collapsibility, rather than arbitrarily assigning a fixed RA pressure. In general, **TR velocity > 2.8 to 2.9 m/s, corresponding to SPAP of approximately 36 mm Hg, assuming an RA pressure of 3 to 5 mm Hg**, indicates elevated RV systolic and PA pressure. SPAP may increase, however, with age and in obesity. In addition, SPAP is also related to stroke volume and systemic blood pressure. Elevated SPAP may not always indicate increased pulmonary vascular resistance (PVR). In general, those who have elevated SPAP should be carefully evaluated. It is important to take into consideration that the RV diastolic function parameters and SPAP are influenced by the systolic and diastolic function of the left heart. PA pressure should be reported along with systemic blood pressure or mean arterial pressure.

Because echocardiography is the first test used in the evaluation of patients presenting with cardiovascular symptoms, it is important to provide basic assessment of right heart structure and function, in ad-

dition to left heart parameters. In those with established right heart failure or pulmonary hypertension (PH), further detailed assessment using other parameters such as PVR, can be carried out.

## OVERVIEW

The right ventricle has long been neglected, yet it is RV function that is strongly associated with clinical outcomes in many conditions. Although the left ventricle has been studied extensively, with established normal values for dimensions, volumes, mass, and function, measures of RV size and function are lacking. The relatively predictable left ventricular (LV) shape and standardized imaging planes have helped establish norms in LV assessment. There are, however, limited data regarding the normal dimensions of the right ventricle, in part because of its complex shape. The right ventricle is composed of 3 distinct portions: the smooth muscular inflow (body), the outflow region, and the trabecular apical region. Volumetric quantification of RV function is challenging because of the many assumptions required. As a result, many physicians rely on visual estimation to assess RV size and function.

The basics of RV dimensions and function were included as part of the ASE and European Association of Echocardiography recommendations for chamber quantification published in 2005.<sup>1</sup> This document, however, focused on the left heart, with only a small section covering the right-sided chambers. Since this publication, there have been significant advances in the echocardiographic assessment of the right heart. In addition, there is a need for greater dissemination of details regarding the standardization of the RV echocardiographic examination.

These guidelines are to be viewed as a starting point to establish a standard uniform method for obtaining right heart images for assessing RV size and function and as an impetus for the development of databases to refine the normal values. This guidelines document is not intended to serve as a detailed description of pathology affecting the right heart, although the document contains many references that describe RV pathologic conditions and how they affect the measurements described.

The purposes of this guidelines document are as follows:

1. Describe the acoustic windows and echocardiographic views required for optimal evaluation of the right heart.
2. Describe the echocardiographic parameters required in routine and directed echocardiographic studies and the views to obtain these parameters for assessing RV size and function.
3. Critically assess the available data from the literature and present the advantages and disadvantages of each measure or technique.
4. Recommend which right-sided measures should be included in the standard echocardiographic report.
5. Provide revised reference values for right-sided measures with cutoff limits representing 95% confidence intervals based on the current available literature.

## METHODOLOGY IN THE ESTABLISHMENT OF REFERENCE VALUE AND RANGES

An extensive systematic literature search was performed to identify all studies reporting echocardiographic right heart measurements in normal subjects. These encompassed studies reporting normal reference values and, more commonly, studies reporting right heart size and



		<ul style="list-style-type: none"> <li>Used for measurement of RV enlargement, RV wall thickness and the RVOT dimension by 2D.</li> <li>View is highly variable depending on transducer angulation and the rib interspace position from which it was obtained. Therefore it should not be the sole view to evaluate RVOT size.</li> </ul>
		<ul style="list-style-type: none"> <li>Shows anterior RVOT in its long-axis view with infundibular segment. The pulmonary valve and main PA are also visible.</li> <li>Used to measure pulmonary annular dimension and to assess pulmonary valve.</li> </ul>
		<ul style="list-style-type: none"> <li>Important view to assess anterior/inferior RV wall and anterior/posterior tricuspid valve leaflets.</li> <li>Anterior and posterior papillary muscles, chordal attachment, and ostium of inferior vena cava including the Eustachian valve are visible. The coronary sinus (not shown) may also be seen in this view.</li> <li>TR jet parameters can be measured in this view provided the TR jet is parallel to the U/S beam.</li> </ul>
		<ul style="list-style-type: none"> <li>Shows the basal anterior RV wall, RVOT, tricuspid valve, pulmonary valve and RA.</li> <li>Normally used to measure RVOT dimension in diastole.</li> <li>TR jet parameters can be measured in this view provided the TR jet is parallel to the U/S beam.</li> <li>Used to assess the interatrial septum for shunts (particularly patent foramen ovale flow just posterior to the aortic root).</li> </ul>
		<ul style="list-style-type: none"> <li>Used to assess the pulmonary valve, pulmonary artery and its branches.</li> <li>Used for measuring pulmonary annulus dimension, pulmonary artery size and for Doppler measurement of the infundibulum, pulmonary valve and pulmonary artery.</li> <li>Proximal and distal RVOT segments are also visible.</li> </ul>
		<ul style="list-style-type: none"> <li>Basal level of anterior, inferior and lateral RV walls.</li> <li>A crescent shape of RV is well appreciated in this view.</li> <li>Septal flattening in systole or diastole from RV volume or pressure overload is often best appreciated in this view.</li> <li>Valuable for initial assessment of RV size, but cannot be used for assessment of RV systolic function due to the asymmetric nature of RV contraction.</li> </ul>
		<ul style="list-style-type: none"> <li>Mid-level of anterior, inferior and lateral RV walls are shown in this view.</li> <li>A crescent shape of RV is well appreciated in this view.</li> <li>Septal flattening in systole or diastole from RV volume or pressure overload is also clearly seen in this view.</li> <li>Valuable for initial assessment of RV size, but cannot be used for assessment of RV systolic function due to the asymmetric nature of RV contraction.</li> </ul>
		<ul style="list-style-type: none"> <li>Useful view for demonstrating RV/RA size, shape and function.</li> <li>Used to measure RV maximal long-axis distance, minor distances at base and mid-level, RV area and RV fractional area change. RA major and minor axis dimensions, RA area and volume are commonly measured here.</li> <li>RV inflow, TR jet by Doppler, tricuspid annulus excursion by M-mode and RV strain by tissue Doppler are also commonly assessed in this view.</li> <li>TR jet parameters can be measured in this view provided the TR jet is parallel to the U/S beam.</li> </ul>
		<ul style="list-style-type: none"> <li>Recommended alternative to Apical 4-chamber to measure RV minor dimension in basal segment of the RV.</li> <li>Useful view for demonstrating RV/RA size, shape and function, with enhanced visualization of the RV free wall.</li> <li>TR jet parameters can be measured in this view provided the TR jet is parallel to the U/S beam.</li> </ul>
		<ul style="list-style-type: none"> <li>This modified 4-chamber view provides information about a portion of the lateral RV wall and oblique plane of the RA.</li> <li>It should <b>not</b> be used quantitatively to assess RA due to its foreshortened and oblique image angle and should <b>not</b> be used for measurement of RV dimensions.</li> <li>It can be used to measure RV inflow parameters and TR parameters provided the TR jet is parallel to the ultrasound beam.</li> <li>ASD and PFO flow can be assessed with 2D and color Doppler.</li> </ul>
		<ul style="list-style-type: none"> <li>Modified view to visualize the anterolateral RV wall.</li> <li>The moderator band is best visualized in this view.</li> <li>TR jet parameters can be measured in this view provided the TR jet is parallel to the U/S beam.</li> </ul>
		<ul style="list-style-type: none"> <li>Modified view to visualize posterolateral RV wall.</li> <li>The coronary sinus is best visualized in this view.</li> <li>TR jet parameters can be measured in this view provided the TR jet is parallel to the U/S beam.</li> </ul>

**Figure 1** Views used to perform comprehensive evaluation of the right heart. Each view is accompanied by uses, advantages, and limitations of that particular view. Ao, aorta; ASD, atrial septal defect; CS, coronary sinus; EF, ejection fraction; EV, Eustachian valve; LA, left atrium; LV, left ventricle; MV, mitral valve; PA, pulmonary artery; PFO, patent foramen ovale; PM, papillary muscle; RA, right atrium; RV, right ventricle; RVOT, right ventricular outflow tract; U/S, ultrasound.

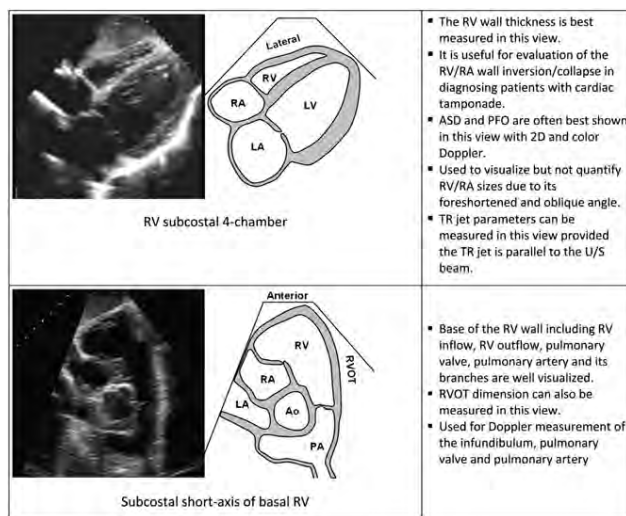


Figure 1 continued

function in patients with specific disease states (eg, chronic obstructive pulmonary disease) versus normal healthy controls. In the latter, only the control group was used in the determination of normal values. It is important to note that these reference values are based on values obtained from *normal individuals* without any history of heart disease and exclude those with history of congenital heart disease. For each measurement, the mean value and standard deviation (SD) were extracted, ensuring that the technique used to obtain the measurement was comparable between studies. Individual patient data were not available and therefore not extracted. The mean values and SDs were pooled and weighted to take into account study size and inter-study variability, as is typical for random-effects meta-analyses. The meta-analysis yielded a pooled estimate for the mean value, a pooled estimate for the lower reference value (ie, mean value  $- 2$  SDs), and a pooled estimate for the upper reference value (ie, mean value  $+ 2$  SDs). In addition, 95% confidence intervals surrounding the mean and upper and lower reference values were calculated to add further insight into the robustness of the reference values. Reference values were reviewed by the writing group members to ensure that they were in accordance with clinical experience, and select measures were further discussed with outside experts. Our document therefore reports the mean values along with the upper and lower reference values in a normal population, each with 95% confidence intervals. Because patient-level data were not available, it is not possible to define cutoffs for body surface area, gender, or ethnicity. As a result, a value may fall within the 95% confidence interval for a given patient, but this value may still be abnormal for that patient, or vice versa. Similarly, patient-level data were not available to divide the abnormal categories into mild, moderate, and severe degrees of abnormality. Interpreters should therefore use their judgment in determining the extent of abnormality observed for any given parameter. In the rare situation in which insufficient data were available to perform the analysis described above, but the committee believed that guidelines were required (eg, estimation of RA pressure), current data were reviewed and a consensus put forth on the basis of the best available data. Many of the values provided in this document are significantly different from those provided in the ASE's guidelines on chamber quantification published in 2005.<sup>1</sup> The prior document's normal values were often based on limited data, at times from a single small study.

Readers are therefore encouraged to use the normal values provided in the current document in the assessment and reporting on right heart size and function.

## ACOUSTIC WINDOWS AND ECHOCARDIOGRAPHIC VIEWS OF THE RIGHT HEART

To differentiate normal RV structure and function from abnormal and to assess RV size, volume, and contractility, a complete set of standardized views must be obtained (Figure 1). These include PLAX, parasternal RV inflow, PSAX, apical 4-chamber, right ventricle–focused apical 4-chamber (Figure 6), and subcostal views. **It is important to use all available views**, because each view adds complementary information, permitting a more complete assessment of the different segments of the right heart chambers. This pertains to the evaluation of both structure and function. For the estimation of RVSP, it is particularly important to interrogate TR by continuous-wave Doppler from all views, because the maximal velocity depends on optimal alignment with the jet. When there are discrepancies in structure and function between different views, the interpreting physician must integrate all information contained within the echocardiographic study to synthesize a global assessment of the right heart. Figure 1 details the standardized right heart views, along with the structures identified in each view.

## NOMENCLATURE OF RIGHT HEART SEGMENTS AND CORONARY SUPPLY

The right coronary artery is the primary coronary supply to the right ventricle via acute marginal branches. In the setting of acute myocardial infarction, in general, the more proximal the occlusion, the more RV myocardium will be affected. In cases of the posterior descending artery occlusion, if there is RV involvement, it may be limited to a portion of the RV inferior wall only, best seen in the RV inflow view. The posterior descending artery gives off perpendicular branches. These posterior septal perforators typically supply the posterior one third of the ventricular septal wall.<sup>2</sup> The blood supply to the moderator band arises from the first septal perforating branch of the left anterior descending coronary artery. This distribution of blood supply may become relevant in cases of alcohol septal ablation. In 30% of hearts, the conus artery arises from a separate coronary ostium and supplies the infundibulum. It may serve as a collateral to the anterior descending artery.<sup>3</sup> In  $<10\%$  of hearts, posterolateral branches of the left circumflex artery supply a portion of the posterior RV free wall.<sup>4,5</sup> The left anterior descending artery may supply a portion of the RV apex, and this segment may be compromised in some cases of left anterior descending artery infarction. In addition, there are certain nonischemic diseases that may be associated with regional wall motion abnormalities of the right ventricle.

## CONVENTIONAL TWO-DIMENSIONAL ASSESSMENT OF THE RIGHT HEART

### A. Right Atrium

The right atrium assists in filling the right ventricle by (1) acting as a reservoir for systemic venous return when the tricuspid valve is closed,



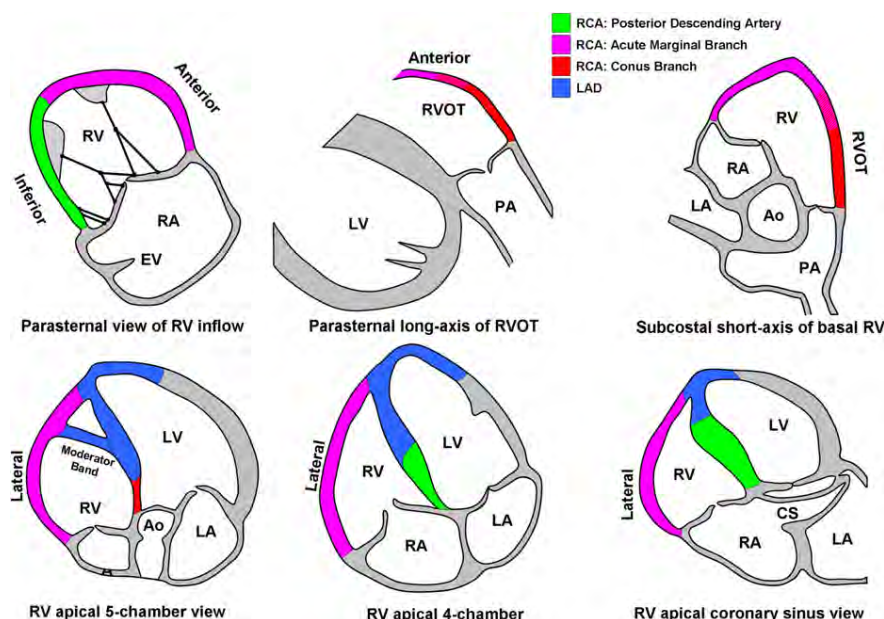


**Figure 2** Segmental nomenclature of the right ventricular walls, along with their coronary supply. Ao, Aorta; CS, coronary sinus; LA, left atrium; LAD, left anterior descending artery; LV, left ventricle; PA, pulmonary artery; RA, right atrium; RCA, right coronary artery; RV, right ventricle; RVOT, right ventricular outflow tract.

(2) acting as a passive conduit in early diastole when the tricuspid valve is open, and (3) acting as an active conduit in late diastole during atrial contraction.<sup>6</sup> To date, only a few studies have focused on the role of the right atrium in disease states.

RA area was a predictor of mortality or transplantation in a study of 25 patients with primary PH. RA dilatation was documented in patients with atrial arrhythmias by both 2D and 3D echocardiography,<sup>7</sup> and reverse remodeling occurred following radiofrequency ablation treatment of atrial fibrillation.<sup>8</sup>

The primary transthoracic window for imaging the right atrium is the apical 4-chamber view. From this window, RA area is estimated by planimetry.<sup>5</sup> The maximal long-axis distance of the right atrium is from the center of the tricuspid annulus to the center of the superior RA wall, parallel to the interatrial septum. A mid-RA minor distance is defined from the mid level of the RA free wall to the interatrial septum, perpendicular to the long axis. RA area is traced at the end of ventricular systole (largest volume) from the lateral aspect of the tricuspid annulus to the septal aspect, excluding the area between the leaflets and annulus, following the RA endocardium, excluding the IVC and superior vena cava and RA appendage (Figure 3).<sup>5</sup> Note that RA dimensions can be distorted and falsely enlarged in patients with chest and thoracic spine deformities.

Normal values for major and minor dimensions and end-systolic area on transthoracic echocardiography are shown in Table 2.

**Advantages:** RA dimensions and area are easily obtained on an apical 4-chamber view and are markers of RA dilatation.

**Disadvantages:** RA area is a more time-consuming measurement than linear dimensions alone but is a better indicator for RV diastolic dysfunction.

**Recommendations:** Images adequate for RA area estimation should be obtained in patients undergoing evaluation for RV or LV dysfunction, using an upper reference limit of 18 cm<sup>2</sup>. RA dimensions should be considered in all patients with significant RV dysfunction in whom image qual-

ity does not permit for the measurement of RA area. Upper reference limits are 4.4 and 5.3 cm for minor-axis and major-axis dimensions, respectively (Table 2). Because of the paucity of standardized RA volume data by 2D echocardiography, routine RA volume measurements are not currently recommended.

**RA Pressure.** RA pressure is most commonly estimated by IVC diameter and the presence of inspiratory collapse.<sup>9</sup> As RA pressure increases, this is transmitted to the IVC, resulting in reduced collapse with inspiration and IVC dilatation. Combining these two parameters results in a good estimation of RA pressure within a limited number of ranges in a majority of patients. Traditional cutoff values for IVC diameter and collapse have recently been revisited, acknowledging that these parameters perform well when estimating low or high RA pressures and less well in intermediate values.<sup>10</sup> Secondary indices of RA pressure may be useful in such scenarios to further refine estimates. In patients being ventilated using positive pressure, the degree of IVC collapse cannot be used to reliably estimate RA pressure, and RA pressure measured by transduction of a central line should be used if available. An IVC diameter  $\leq$  12 mm in these patients, however, appears accurate in identifying patients with RA pressures  $<$  10 mm Hg.<sup>11</sup> In this same patient group, if the IVC is small and collapsed, this suggests hypovolemia.

The subcostal view is most useful for imaging the IVC, with the IVC viewed in its long axis.<sup>12</sup> The measurement of the IVC diameter should be made at end-expiration and just proximal to the junction of the hepatic veins that lie approximately 0.5 to 3.0 cm proximal to the ostium of the right atrium (Figure 4).<sup>13,14</sup> To accurately assess IVC collapse, the change in diameter of the IVC with a sniff and also with quiet respiration should be measured, ensuring that the change in diameter does not reflect a translation of the IVC into another plane.<sup>4,5,12</sup> It may be better to view the IVC in the cross-sectional view to make sure that the long-axis view is perpendicular

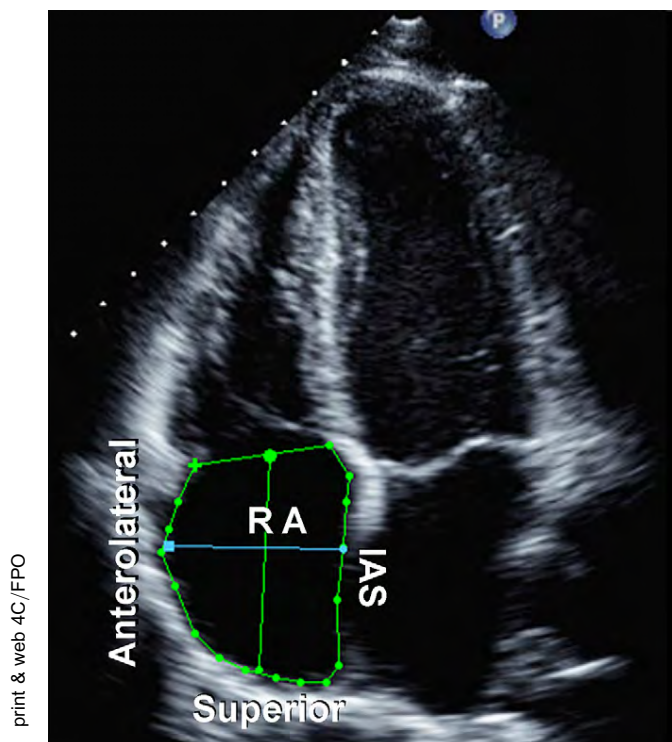


**Figure 3** Tracing of the right atrium (RA) is performed from the plane of the tricuspid annulus (TA), along the interatrial septum (IAS), superior and anterolateral walls of the RA. The right atrial major dimension is represented by the *green line* from the TA center to the superior right atrial wall, and the right atrial minor dimension is represented by the *blue line* from the anterolateral wall to the IAS.

to it. Although a distended IVC usually denotes elevated RA pressures, in patients with otherwise normal exam results, reassessing the IVC size and collapsibility in the left lateral position may be useful to avoid the potentially erroneous inference of increased RA filling pressure. The IVC may also be dilated in normal young athletes, and in this population, it may not reflect elevated RA pressure.

Hepatic vein flow patterns provide complementary insights into RA pressure. At low or normal RA pressures, there is systolic predominance in hepatic vein flow, such that the velocity of the systolic wave ( $V_s$ ) is greater than the velocity of the diastolic wave ( $V_d$ ). At elevated RA pressures, this systolic predominance is lost, such that  $V_s$  is substantially decreased and  $V_s/V_d$  is  $<1$ . The hepatic vein systolic filling fraction is the ratio  $V_s/(V_s + V_d)$ , and a value  $<55\%$  was found to be the most sensitive and specific sign of elevated RA pressure.<sup>15</sup> Importantly, hepatic vein flow velocities have been validated in mechanically ventilated patients, provided that the velocities are averaged over  $\geq 5$  consecutive beats and comprising  $\geq 1$  respiratory cycle.

Other 2D signs of increased RA pressure include a dilated right atrium and an interatrial septum that bulges into the left atrium throughout the cardiac cycle. These are qualitative and comparative, and do not allow the interpreter to assign an RA pressure but if present should prompt a more complete evaluation of RA pressure as well as a search for possible etiologies.

**Advantages:** IVC dimensions are usually obtainable from the subcostal window.

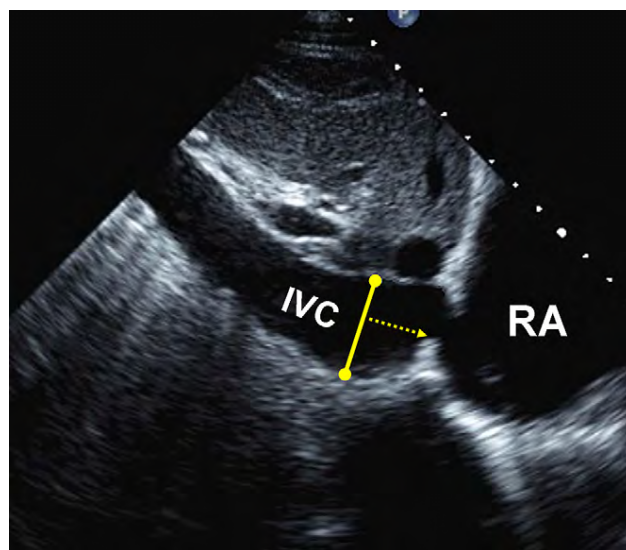


**Figure 4** Inferior vena cava (IVC) view. Measurement of the IVC. The diameter (*solid line*) is measured perpendicular to the long axis of the IVC at end-expiration, just proximal to the junction of the hepatic veins that lie approximately 0.5 to 3.0 cm proximal to the ostium of the right atrium (RA).

**Disadvantages:** IVC collapse does not accurately reflect RA pressure in ventilator-dependent patients. It is less reliable for intermediate values of RA pressure.

**Recommendations:** For simplicity and uniformity of reporting, specific values of RA pressure, rather than ranges, should be used in the determination of SPAP. IVC diameter  $\leq 2.1$  cm that collapses  $>50\%$  with a sniff suggests a normal RA pressure of 3 mm Hg (range, 0–5 mm Hg), whereas an IVC diameter  $> 2.1$  cm that collapses  $<50\%$  with a sniff suggests a high RA pressure of 15 mm Hg (range, 10–20 mm Hg). In indeterminate cases in which the IVC diameter and collapse do not fit this paradigm, an intermediate value of 8 mm Hg (range, 5–10 mm Hg) may be used, or, preferably, secondary indices of elevated RA pressure should be integrated. These include restrictive right-sided diastolic filling pattern, tricuspid E/E' ratio  $> 6$ , and diastolic flow predominance in the hepatic veins (which can be quantified as a systolic filling fraction  $< 55\%$ ). In indeterminate cases, if none of these secondary indices of elevated RA pressure are present, RA pressure may be downgraded to 3 mm Hg. If there is minimal IVC collapse with a sniff ( $<35\%$ ) and secondary indices of elevated RA pressure are present, RA pressure may be upgraded to 15 mm Hg. If uncertainty remains, RA pressure may be left at the intermediate value of 8 mm Hg. In patients who are unable to adequately perform a sniff, an IVC that collapses  $< 20\%$  with quiet inspiration suggests elevated RA pressure. This method of assigning an RA pressure is preferable to assuming a fixed RA pressure value for all patients.

#### B. Right Ventricle

**RV Wall Thickness.** RV wall thickness is a useful measurement for RVH, usually the result of RVSP overload.<sup>16–18</sup> Increased RV thickness can be seen in infiltrative and hypertrophic cardiomyopathies, as well



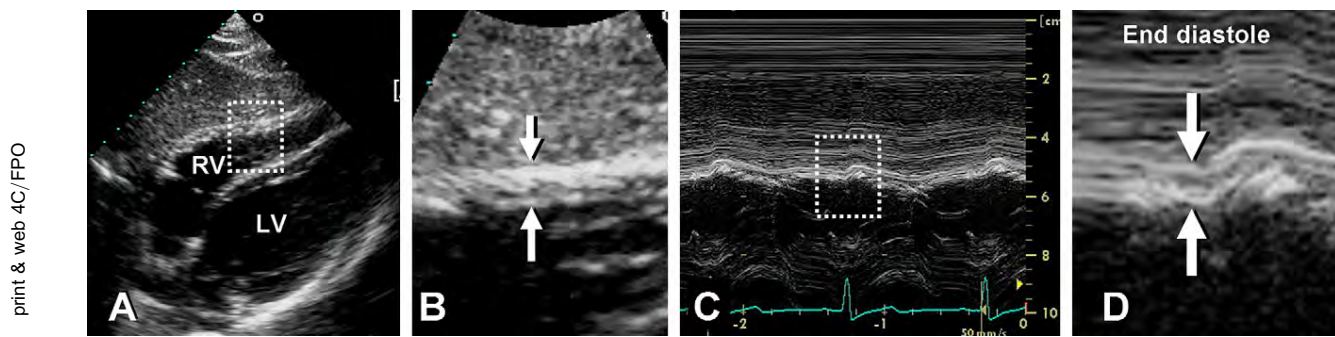


**Figure 5** Measurement of end-diastolic right ventricular wall thickness. (A) Subcostal 2-dimensional image of right ventricular wall. (B) Zoom of region outlined in (A) with right ventricular wall thickness indicated by arrows. (C) M-mode image corresponding to arrows in (B). (D) Zoom of region outlined in (C) with arrows indicating wall thickness at end-diastole.

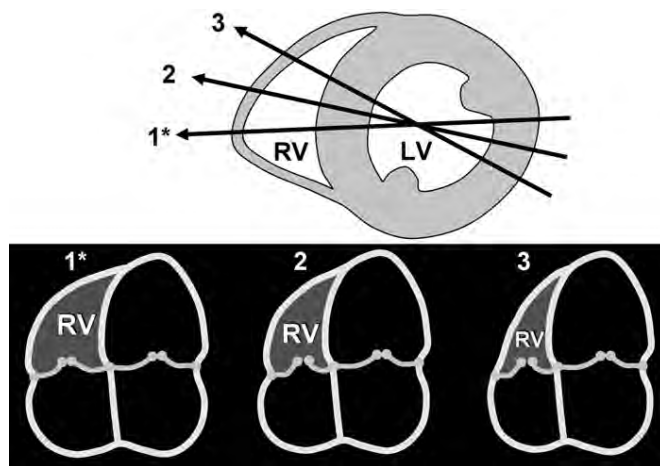


**Figure 6** Diagram showing the recommended apical 4-chamber (A4C) view with focus on the right ventricle (RV) (1\*) and the sensitivity of right ventricular size with angular change (2,3) despite similar size and appearance of the left ventricle (LV). The lines of intersection of the A4C planes (1\*,2,3) with a mid left ventricular short-axis are shown above and corresponding A4C views below.

as in patients with significant LV hypertrophy, even in the absence of PH.<sup>19</sup> RV free wall thickness can be measured at end-diastole by M-mode or 2D echocardiography from the subcostal window, preferably at the level of the tip of the anterior tricuspid leaflet or left parasternal windows.<sup>4,16</sup> From the subcostal view, one can align the ultrasound beam perpendicular to the RV free wall. Excluding RV trabeculations and papillary muscle from RV endocardial border is critical for accurately measuring the RV wall thickness. Moving the focus to the RV wall region and decreasing the depth will improve the endocardial border definition. Every effort must be made to exclude epicardial fat to avoid erroneously increased measurements. When image quality permits, fundamental imaging should be used to avoid the increased structure thickness seen with harmonic imaging. When there is significant thickening of the visceral pericardium, the measurement of the RV wall may be challenging.

Certain conditions are associated with RV wall thinning, such as Uhl anomaly or arrhythmogenic RV cardiomyopathy. There are no accepted echocardiographic criteria to define an abnormally thin RV wall.

**Advantages:** RV wall thickness can be measured by M-mode or 2D echocardiography from either the subcostal or left parasternal window.

**Disadvantages:** There is a lack of established prognostic information.

**Recommendations:** Abnormal RV wall thickness should be reported, if present, in patients suspected of having RV and/or LV dysfunction, using the normal cut-off of 0.5 cm from either PLAX or subcostal windows (Table 2).

**RV Linear Dimensions.** The right ventricle dilates in response to chronic volume and/or pressure overload<sup>20</sup> and with RV failure.<sup>21</sup> Indexed RV end-diastolic diameter has been identified as a predictor of survival in patients with chronic pulmonary disease,<sup>22</sup> and the RV/LV end-diastolic diameter ratio was shown to be a predictor of adverse clinical events and/or hospital survival in patients with acute pulmonary embolism.<sup>23,24</sup> Correlation of RV linear dimensions with RV end-diastolic volumes appears to worsen with increased preload<sup>25</sup> or afterload.<sup>26</sup>

Using 2D echocardiography, RV size can be measured from a 4-chamber view obtained from the apical window at end-diastole. Although quantitative validation is lacking, qualitatively, the right ventricle should appear smaller than the left ventricle and usually no more than two thirds the size of the left ventricle in the *standard* apical 4-chamber view. If the right ventricle is larger than the left ventricle in this view, it is likely significantly enlarged. This may be applied to certain conditions such as severe RV pressure or volume overload, in which the right ventricle may measure within the normal reference limits but appears larger than the small, underfilled left ventricle. In the standard transthoracic apical 4-chamber window, the left ventricle is considered the “apex-forming” ventricle. As the right ventricle enlarges, it may displace the left ventricle and occupy the apex. This usually signifies that the right ventricle is at least moderately dilated, though this finding has not been validated quantitatively.

One major limitation of RV imaging by transthoracic echocardiography is the result of a lack of fixed reference points to ensure optimization of the right ventricle. As a result, the imager can image the RV through various cut planes, resulting in a normal, medium, or smaller dimension (Figure 6). As a result, it is critical to attempt to adjust the apical 4-chamber to acquire the “right ventricle-focused view,” as detailed below. To optimize imaging of the RV lateral wall, the 4-chamber image may require adjustment from its usual attention on the left ventricle to a focus on the right ventricle. To avoid underestimating the minor distance, the transducer is rotated until the maximal plane is obtained. To avoid overestimation, the transducer must be properly positioned over the cardiac apex with the plane through

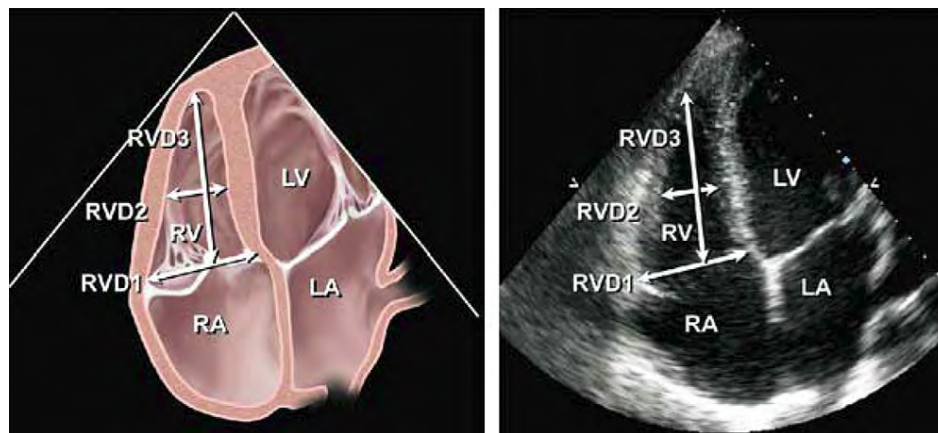


**Figure 7** Diagram (*left*) and corresponding echocardiographic apical 4-chamber image (*right*) showing the right ventricular (RV) basal (RVD1) and mid cavity (RVD2) RV minor dimensions and the RV longitudinal dimension (RVD3). The transducer is adjusted to focus on the RV chamber, with the goal of maximizing RV chamber size. The RV free wall is better seen in this view, also facilitating measurements for fractional area change. Reproduced from *J Am Soc Echocardiogr*.<sup>1</sup>

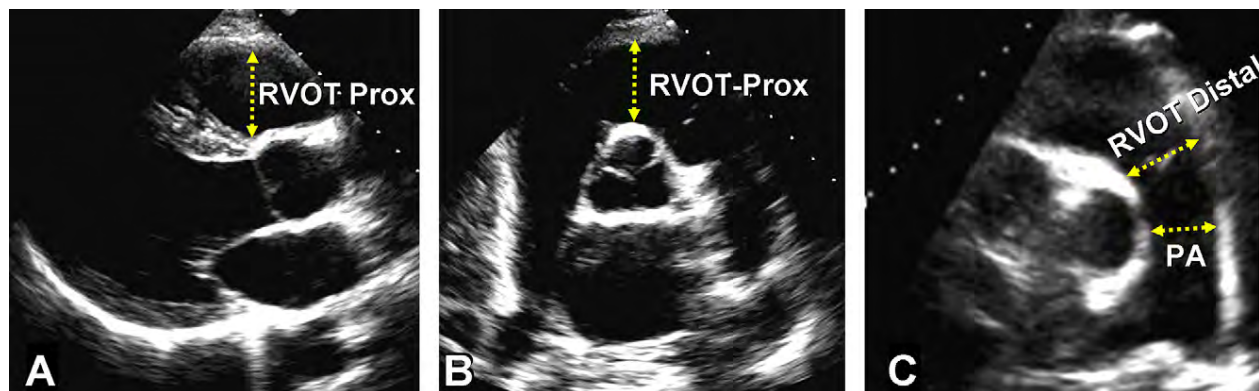


**Figure 8** Measurement of right ventricular outflow tract (RVOT) dimensions at the proximal or subvalvular level (RVOT-Prox) and at the distal or pulmonic valve (RVOT-Distal) in the (A) parasternal long-axis RVOT anterior portion view, (B) basal parasternal short-axis view, and (C) parasternal short-axis of pulmonary bifurcation view. PA, Pulmonary artery dimension between valve and the bifurcation point.

the left ventricle in the center of the cavity. One must ensure that the RV is not foreshortened and that the LV outflow tract is not opened up (avoid the apical 5-chamber view).

The basal and mid cavity RV diameters, as well as the RV longitudinal dimension, may be obtained (Figure 7).<sup>1</sup> The basal diameter is generally defined as the maximal short-axis dimension in the basal one third of the right ventricle seen on the 4-chamber view.<sup>1,25,27</sup> In the normal right ventricle, the maximal short-axis dimension is usually located in the basal one third of the ventricular cavity.<sup>4,25</sup> The mid cavity diameter is measured in the middle third of the right ventricle at the level of the LV papillary muscles. The longitudinal dimension is drawn from the plane of the tricuspid annulus to the RV apex. Note that RV dimensions can be distorted and falsely enlarged in patients with chest and thoracic spine deformities.

**Advantages:** RV linear dimensions are easily obtained on an apical 4-chamber view and are markers of RV dilatation.

**Disadvantages:** RV dimensions are highly dependent on probe rotation by the user, which can result in an underestimation of RV width.

**Recommendations: Patients with echocardiographic evidence of right-sided heart disease or PH should ideally have measurements of RV basal, mid cavity, and longitudinal dimensions on a 4-chamber view. In all complete echocardiographic studies, the RV basal measurement should be reported, and the report should state the window from which the measurement was performed (ideally the right ventricle-focused view), to permit interstudy comparisons. The relative size of the right ventricle should be compared with that of the LV to help the study interpreter determine if there is RV dilatation, and the interpreter may report the right ventricle as dilated despite measuring within the normal range, on the basis of a right ventricle appearing significantly larger than the left ventricle. The upper reference limit for the RV basal dimension is 4.2 cm (Table 2).**

#### C. RVOT

The RVOT is generally considered to include the subpulmonary infundibulum, or conus, and the pulmonary valve. The subpulmonary

**Table 2** Chamber dimensions

Dimension	Studies	n	LRV (95% CI)	Mean (95% CI)	URV (95% CI)
RV mid cavity diameter (mm) (Figure 7, RVD2)	12	400	20 (15-25)	28 (23-33)	35 (30-41)
RV basal diameter (mm) (Figure 7, RVD1)	10	376	24 (21-27)	33 (31-35)	42 (39-45)
RV longitudinal diameter (mm) (Figure 7, RVD3)	12	359	56 (50-61)	71 (67-75)	86 (80-91)
RV end-diastolic area (cm <sup>2</sup> ) (Figure 9)	20	623	10 (8-12)	18 (16-19)	25 (24-27)
RV end-systolic area (cm <sup>2</sup> ) (Figure 9)	16	508	4 (2-5)	9 (8-10)	14 (13-15)
RV end-diastolic volume indexed (mL/m <sup>2</sup> )	3	152	44 (32-55)	62 (50-73)	80 (68-91)
RV end-systolic volume indexed (mL/m <sup>2</sup> )	1	91	19 (17-21)	33 (31-34)	46 (44-49)
3D RV end-diastolic volume indexed (mL/m <sup>2</sup> )	5	426	40 (28-52)	65 (54-76)	89 (77-101)
3D RV end-systolic volume indexed (mL/m <sup>2</sup> )	4	394	12 (1-23)	28 (18-38)	45 (34-56)
RV subcostal wall thickness (mm) (Figure 5)	4	180	4 (3-4)	5 (4-5)	5 (5-6)
RVOT PLAX wall thickness (mm) (not shown)	9	302	2 (1-2)	3 (3-4)	5 (4-6)
RVOT PLAX diameter (mm) (Figure 8)	12	405	18 (15-20)	25 (23-27)	33 (30-35)
RVOT proximal diameter (mm) (Figure 8, RVOT-Prox)	5	193	21 (18-25)	28 (27-30)	35 (31-39)
RVOT distal diameter (mm) (Figure 8, RVOT-Distal)	4	159	17 (12-22)	22 (17-26)	27 (22-32)
RA major dimension (mm) (Figure 3)	8	267	34 (32-36)	44 (43-45)	53 (51-55)
RA minor dimension (mm) (Figure 3)	16	715	26 (24-29)	35 (33-37)	44 (41-46)
RA end-systolic area (cm <sup>2</sup> ) (Figure 3)	8	293	10 (8-12)	14 (14-15)	18 (17-20)

CI, Confidence interval; LRV, lower reference value; PLAX, parasternal long-axis; RA, right atrial; RV, right ventricular; RVD, right ventricular diameter; RVOT, right ventricular outflow tract; 3D, three-dimensional; URV, upper reference value.

**Table 3** Estimation of RA pressure on the basis of IVC diameter and collapse

Variable	Normal (0-5 [3] mm Hg)	Intermediate (5-10 [8] mm Hg)		High (15 mm Hg)
IVC diameter	≤2.1 cm	≤2.1 cm	>2.1 cm	>2.1 cm
Collapse with sniff	>50%	<50%	>50%	<50%
Secondary indices of elevated RA pressure				<ul style="list-style-type: none"> <li>• Restrictive filling</li> <li>• Tricuspid E/E' &gt; 6</li> <li>• Diastolic flow predominance in hepatic veins (systolic filling fraction &lt; 55%)</li> </ul>

Ranges are provided for low and intermediate categories, but for simplicity, midrange values of 3 mm Hg for normal and 8 mm Hg for intermediate are suggested. Intermediate (8 mm Hg) RA pressures may be downgraded to normal (3 mm Hg) if no secondary indices of elevated RA pressure are present, upgraded to high if minimal collapse with sniff (<35%) and secondary indices of elevated RA pressure are present, or left at 8 mm Hg if uncertain.

IVC, Inferior vena cava; RA, right atrial.

infundibulum is a cone-shaped muscular structure that extends from the crista supraventricularis to the pulmonary valve. It is distinct from the rest of the right ventricle in origin<sup>28</sup> and anatomy.<sup>29</sup> The delay in regional activation of the RVOT contributes to the peristalsis-like contraction pattern of the normal right ventricle.<sup>29,30</sup> The role of the RVOT is particularly important in some patients with congenital heart disease<sup>31</sup> or arrhythmia,<sup>32</sup> and the RVOT is often the first segment of the right ventricle to show diastolic inversion in the setting of tamponade.

The RVOT is best viewed from the left parasternal and subcostal windows, but it also may be evaluated from the apical window in thin individuals or adults with large rib spaces. The size of the RVOT should be measured at end-diastole on the QRS deflection. In the PLAX view, a portion of the proximal RVOT can be measured (RVOT-Prox in Figure 8A). In the short-axis view, the RVOT linear dimension can be measured from (1) the anterior aortic wall to the RV free wall above the aortic valve (RVOT-Prox in Figure 8B) and (2) just proximal to the pulmonary valve (RVOT-Distal in Figure 8C).<sup>1</sup> This latter site, at the connection of the RV infundibulum with the pulmonary valve is preferred, especially when measuring right-sided stroke

volume for the calculation of Qp/Qs or regurgitant fraction. The PLAX view of the RVOT is used in particular in the evaluation of arrhythmogenic RV dysplasia.<sup>33</sup> With transesophageal echocardiography, the RVOT is well visualized in the midesophageal RV inflow-outflow view. The use of 3D echocardiography has been shown to be helpful in the assessment of the RVOT.<sup>34</sup> Note that RVOT dimensions can be distorted and falsely enlarged in patients with chest and thoracic spine deformities.

**Advantages:** RVOT dimensions are easily obtained from the left PSAX window. Certain lesions may primarily affect the RVOT.

**Disadvantages:** Limited normative data are available. The window for measurement of RVOT size has not been standardized, and oblique imaging of the RVOT may underestimate or overestimate its size. The endocardial definition of the anterior wall is often suboptimal.

**Recommendations:** In studies on select patients with congenital heart disease or arrhythmia potentially involving the RVOT, proximal and distal diameters of the RVOT should be measured from the PSAX or PLAX views. The PSAX distal RVOT diameter, just proximal to the



print & web 4C/FPO

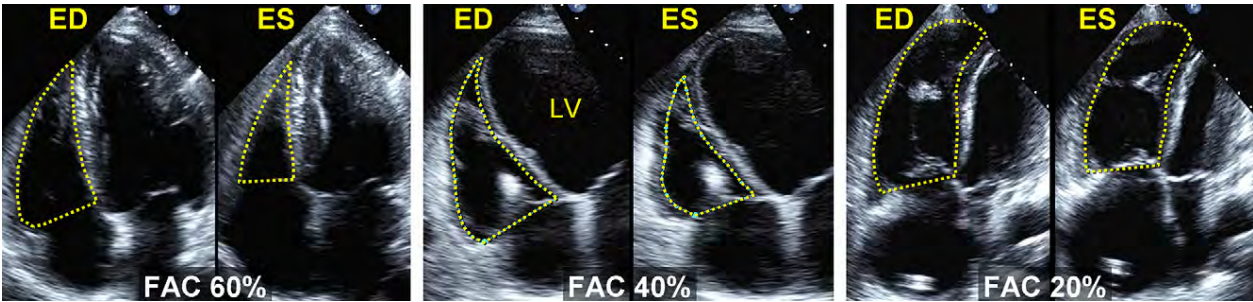


**Figure 9** Examples of right ventricular fractional area change (FAC). Percentage FAC =  $100 \times \text{end-diastolic area (AreaED)} - \text{end-systolic area (Area ES)}/\text{end-diastolic area}$ . The endocardial border is traced in apical 4-chamber (A4C) views from the tricuspid annulus along the free wall to the apex, then back to the annulus, along the interventricular septum at end-diastole (ED) and end-systole (ES). Trabeculation, tricuspid leaflets, and chords are included in the chamber. (Left) Normal subject, FAC 60%. (Middle) Moderately dilated right ventricle (RV), FAC 40%, and a markedly dilated left ventricle (LV). (Right) Dilated RV, FAC 20%, and the LV is foreshortened as a result of optimizing the view for the right ventricular chamber.

**Table 4** Systolic function

Variable	Studies	n	LRV (95% CI)	Mean (95% CI)	URV (95% CI)
TAPSE (mm) (Figure 17)	46	2320	16 (15-18)	23 (22-24)	30 (29-31)
Pulsed Doppler velocity at the annulus (cm/s)	43	2139	10 (9-11)	15 (14-15)	19 (18-20)
Color Doppler velocities at the annulus (cm/s)	5	281	6 (5-7)	10 (9-10)	14 (12-15)
Pulsed Doppler MPI (Figures 16 and 18)	17	686	0.15 (0.10-0.20)	0.28 (0.24-0.32)	0.40 (0.35-0.45)
Tissue Doppler MPI (Figure 18)	8	590	0.24 (0.16-0.32)	0.39 (0.34-0.45)	0.55 (0.47-0.63)
FAC (%) (Figure 8)	36	1276	35 (32-38)	49 (47-51)	63 (60-65)
RV EF (%) (Figure 8)	12	596	44 (38-50)	58 (53-63)	71 (66-77)
3D RV EF (%)	9	524	44 (39-49)	57 (53-61)	69 (65-74)
IVA (m/s <sup>2</sup> )	12	389	2.2 (1.4-3.0)	3.7 (3.0-4.4)	5.2 (4.4-5.9)

CI, Confidence interval; EF, ejection fraction; FAC, fractional area change; IVA, isovolumic acceleration; LRV, lower reference value; MPI, myocardial performance index; RV, right ventricular; TAPSE, tricuspid annular plane systolic excursion; 3D, three-dimensional; URV, upper reference value.

pulmonary annulus, is the most reproducible and should be generally used. For select cases such as suspected arrhythmogenic RV cardiomyopathy, the PLAX measure may be added. The upper reference limit for the PSAX distal RVOT diameter is 27 mm and for PLAX is 33 mm (Table 2).

**FRACTIONAL AREA CHANGE AND VOLUMETRIC ASSESSMENT OF THE RIGHT VENTRICLE**

**A. RV Area and FAC**

The percentage RV FAC, defined as (end-diastolic area – end-systolic area)/end-diastolic area  $\times$  100, is a measure of RV systolic function that has been shown to correlate with RV EF by magnetic resonance imaging (MRI).<sup>25,35</sup> RV FAC was found to be an independent predictor of heart failure, sudden death, stroke, and/or mortality in studies of patients after pulmonary embolism<sup>36</sup> and myocardial infarction.<sup>37,38</sup> FAC is obtained by tracing the RV endocardium both in systole and diastole from the annulus, along the free wall to the apex, and then back to the annulus, along the interventricular septum. Care must be taken to trace the free wall beneath the trabeculations (Figure 9).

**Recommendations: Two-dimensional Fractional Area Change is one of the recommended methods of quantitatively estimating RV function, with a lower reference value for normal RV systolic function of 35%.**

**B. Two-Dimensional Volume and EF Estimation**

The complexity of estimating RV volume and function with 2D echocardiography has been well documented, and interested readers are referred to reviews for a more complete discussion.<sup>29,39,40</sup> In brief, the 2D echocardiographic methods of calculating RV volume can be divided into area-length methods, disk summation methods, and other methods.

The area-length methods, initially adopted for biplane angiography, require an approximation of RV geometry, most commonly based on modified pyramidal or ellipsoidal models.<sup>39,41,42</sup> It underestimates MRI-derived RV volume and is inferior in comparison with 3D echocardiographic methods of RV volume estimation.<sup>43</sup>

The disk summation method has also been applied to determine a RV “body” volume, using predominantly the apical 4-chamber view.<sup>44</sup> RV volumes are therefore underestimated because of the exclusion of the RVOT and technical limitations of the echocardiographic images.

RV EF from 2D methods is calculated as (end-diastolic volume – end-systolic volume)/end-diastolic volume. The lower reference limit



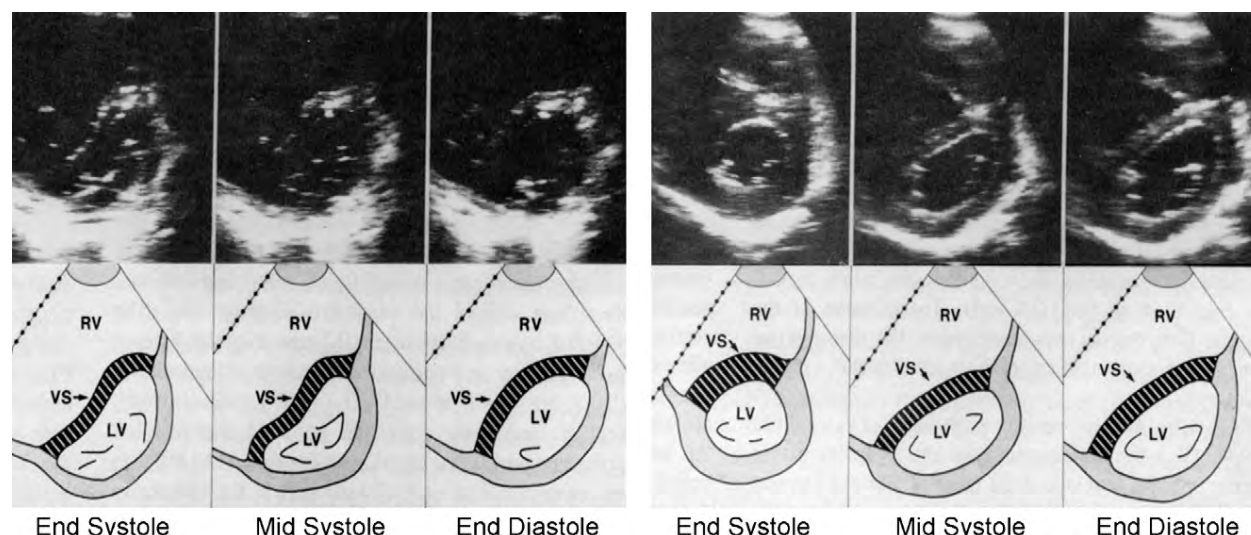


**Figure 10** Serial stop-frame short-axis two-dimensional echocardiographic images of the left ventricle at the mitral chordal level with diagrams from a patient with isolated right ventricular (RV) pressure overload due to primary pulmonary hypertension (*left*) and from a patient with isolated RV volume overload due to tricuspid valve resection (*right*). Whereas the left ventricular (LV) cavity maintains a circular profile throughout the cardiac cycle in normal subjects, in RV pressure overload there is leftward ventricular septal (VS) shift and reversal of septal curvature present throughout the cardiac cycle with most marked distortion of the left ventricle at end-systole. In the patient with RV volume overload, the septal shift and flattening of VS curvature occurs predominantly in mid to late diastole with relative sparing of LV deformation at end-systole. Reproduced with permission from *J Am Coll Cardiol*.<sup>69</sup>

of pooled studies using these methods for the measurement of RV EF is 44%, with a 95% confidence interval of 38% to 50% (Table 4).

**Recommendations: Two dimensionally derived estimation of RV EF is not recommended, because of the heterogeneity of methods and the numerous geometric assumptions.**

### C. Three-Dimensional Volume Estimation

The accuracy of RV volumes on 3D echocardiography has been validated against animal specimens,<sup>45,46</sup> animal cast models of the right ventricle,<sup>46-48</sup> and human intraoperative RV volume measurements.<sup>49</sup> At present, the disk summation and apical rotational methods for RV volume and EF calculation are most commonly used in 3D echocardiography. Images may be acquired by transesophageal echocardiography<sup>49-51</sup> as well as transthoracic echocardiography. The methodology is complex and beyond the scope of this document, and interested readers are referred to a recent report by Horton et al<sup>52</sup> for a discussion of methodology. Compared in vitro, the 3D apical rotational method was most accurate when  $\geq 8$  equiangular planes were analyzed.<sup>46</sup> Three-dimensional apical rotation using 8 imaging planes provided similar results to the 3D disk summation method in a mixed adult patient group.<sup>53</sup> In a variety of clinical settings, both methods have shown to correlate well with MRI-derived RV volumes in children<sup>54-56</sup> and adults.<sup>51,57-63</sup>

With 3D echocardiography, there is less underestimation of RV end-diastolic and end-systolic volumes and improved test-retest variability compared with 2D echocardiography.<sup>43,60</sup> Pooled data from several small studies and one larger study<sup>64</sup> indicate that the upper reference limit for indexed RV end-diastolic volume is 89 mL/m<sup>2</sup> and for end-systolic volume is 45 mL/m<sup>2</sup>, with indexed volumes being 10% to 15% lower in women than in men (Table 2). The lower reference limit for RV EF is 44% (Table 4).

**Advantages:** RV volumes and EF may be accurately measured by 3D echocardiography using validated real-time 3D algorithms.

**Disadvantages:** Limited normative data are available, with studies using different methods and small numbers of subjects. RV volumes by both 2D and 3D echocardiography tend to underestimate MRI-derived RV volumes, although 3D methods are more accurate. Moreover, the 3D disk summation method is a relatively time-consuming measurement to make. Finally, fewer data are available in significantly dilated or dysfunctional ventricles, making the accuracy of 3D volumes and EFs less certain.

**Recommendations: In studies in selected patients with RV dilatation or dysfunction, 3D echocardiography using the disk summation method may be used to report RV EFs. A lower reference limit of 44% has been obtained from pooled data. Until more studies are published, it may be reasonable to reserve 3D methods for serial volume and EF determinations.**

### THE RIGHT VENTRICLE AND INTERVENTRICULAR SEPTAL MORPHOLOGY

Chronic dilatation of the right ventricle such as may occur with isolated RV volume overload (eg, TR) results in progressive lengthening of the base to apex as well as the free wall to septum dimensions of the right ventricle, with the RV apex progressively replacing the left ventricle as the true apex of the heart. In the PSAX, the left ventricle assumes a progressively more *D-shaped* cavity as the ventricular septum flattens and progressively loses its convexity with respect to the center of the RV cavity during diastole.<sup>65-67</sup> RV pressure overload also distorts the normal circular short-axis geometry of the left ventricle by shifting the septum leftward away from the center of the right ventricle and toward the center of the left ventricle, resulting in

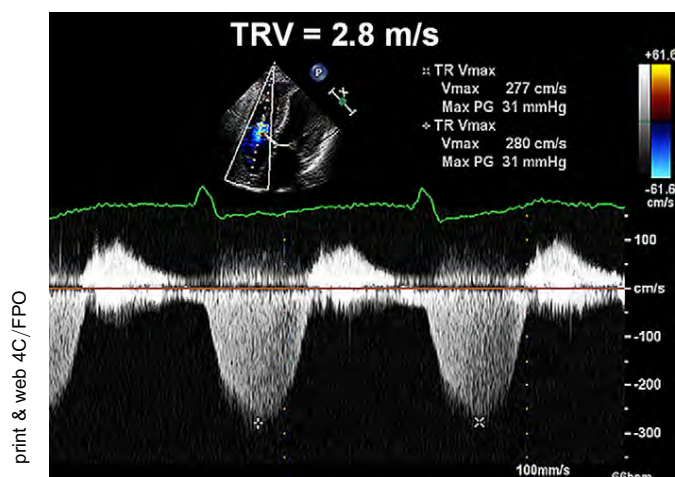


**Figure 11** Doppler echocardiographic determination of systolic pulmonary artery pressure (SPAP). Spectral continuous-wave Doppler signal of tricuspid regurgitation corresponding to the right ventricular (RV)–right atrial (RA) pressure gradient. SPAP was calculated as the sum of the estimated RA pressure (RAP) and the peak pressure gradient between the peak right ventricle and the right atrium, as estimated by application of the modified Bernoulli equation to peak velocity represented by the tricuspid regurgitation Doppler signal. In this example, SPAP is estimated at 31 + central venous pressure, or 34 mm Hg, if RAP is assumed to be 3 mm Hg. Adapted with permission from *J Am Soc Echocardiogr*.<sup>52</sup>

flattening of the ventricular septum and a *D-shaped* short-axis LV cavity profile predominantly during systole. This relationship between the left ventricle and right ventricle can be quantitated on the basis of the ratio between the LV anteroposterior dimension and the septolateral dimension. This “eccentricity index” is abnormal and suggests RV overload when this ratio is  $>1.0$ .<sup>68</sup> The configuration of the interventricular septum is dependent on the relative pressure gradient between the right ventricle and left ventricle at each stage of the cardiac cycle. Because the majority of RV pressure overload conditions in adults arise secondary to the effects of elevation in LV filling pressure, the analysis of ventricular septal geometry and interaction is complicated by the superimposition of systolic RV pressure overload and diastolic LV pressure overload in these patients.<sup>69</sup>

#### A. Differential Timing of Geometric Distortion in RV Pressure and Volume Overload States

Differences in the timing of ventricular septal motion have been measured with Doppler tissue imaging and M-mode echocardiography (Figure 10).<sup>70</sup> Although patients with relatively isolated RV volume overload have the most marked shift of the ventricular septum away from the center of the right ventricle at end-diastole (with relatively more normal septal geometry at end-systole), patients with relatively isolated RV pressure overload have leftward septal shift away from the center of the right ventricle at both end-systole and end-diastole, with the most marked deformation at end-systole. In selected patient populations such as PA hypertension, the ventricular septal eccentricity index and its timing can be quantitated to provide prognostic information that tracks clinical responses to effective therapies.<sup>71,72</sup> Analysis of septal motion is best performed in the absence of significant conduction delays, particularly left bundle branch block.

**Recommendations:** Visual assessment of ventricular septal curvature looking for a D-shaped pattern in systole and diastole should be used to help in the diagnosis of RV volume and/or pressure overload. Although a D-shaped septum is not diagnostic in RV overload, with its presence, additional emphasis should be placed on the confirmation, as well as determination, of the etiology and severity of right-sided pressure and/or volume overload.

### HEMODYNAMIC ASSESSMENT OF THE RIGHT VENTRICLE AND PULMONARY CIRCULATION

#### A. Systolic Pulmonary Artery Pressure

SPAP can be estimated using TR velocity, and PADP can be estimated from the end-diastolic pulmonary regurgitation velocity. Mean PA pressure can be estimated by the PA acceleration time (AT) or derived from the systolic and diastolic pressures.

RVSP can be reliably determined from peak TR jet velocity, using the simplified Bernoulli equation and combining this value with an estimate of the RA pressure:  $RVSP = 4(V)^2 + RA \text{ pressure}$ , where  $V$  is the peak velocity (in meters per second) of the tricuspid valve regurgitant jet, and RA pressure is estimated from IVC diameter and respiratory changes as described above. In the absence of a gradient of across the pulmonic valve or RVOT, SPAP is equal to RVSP. In cases in which RVSP is elevated, obstruction at the level of the RVOT or pulmonic valve should be excluded, especially in patients with congenital heart disease or post-pulmonic valve surgery. The simplified Bernoulli equation may occasionally underestimate the RV-RA gradient because of its neglect of the inertial component of the complete Bernoulli equation. Because velocity measurements are angle dependent, it is recommended to gather TR signals from several windows and to use the signal with the highest velocity.

Technically adequate signals with well-defined borders can be obtained in the majority of patients. It is recommended that Doppler sweep speeds of 100 mm/s be used for all tracings. If the signal is weak, it may be enhanced with agitated saline or blood-saline contrast, but it is important to avoid overestimation of the spectral envelope by ensuring that only the well-defined, dense spectral profile is measured. This is important both with and without contrast (Figure 12).

The normal cutoff value for invasively measured mean PA pressure is 25 mmHg. In the echocardiography laboratory, SPAP is more commonly measured and reported. Normal resting values are usually defined as a peak TR gradient of  $\leq 2.8$  to 2.9 m/s or a peak systolic pressure of 35 or 36 mm Hg, assuming an RA pressure of 3 to 5 mm Hg.<sup>73</sup> This value may increase with age and increasing body surface area and this should be considered when estimations are at the upper limits of normal.<sup>74,75</sup> The most recent American College of Cardiology Foundation and American Heart Association expert consensus document on PH recommends further evaluation of patients with dyspnea with estimated RVSP  $> 40$  mm Hg.<sup>76</sup> Some cardiologists who care for patients with congenital heart disease will consider SPAP greater than two thirds of the systemic blood pressure as indicative of severe PH.

Determination of SPAP by the sum of peak RV-RA gradient and RA pressure has been established as a reliable method since the publication by Yock and Popp<sup>77</sup> in 1984 and has been proven by other studies,<sup>78</sup> but additional studies have questioned the accuracy of

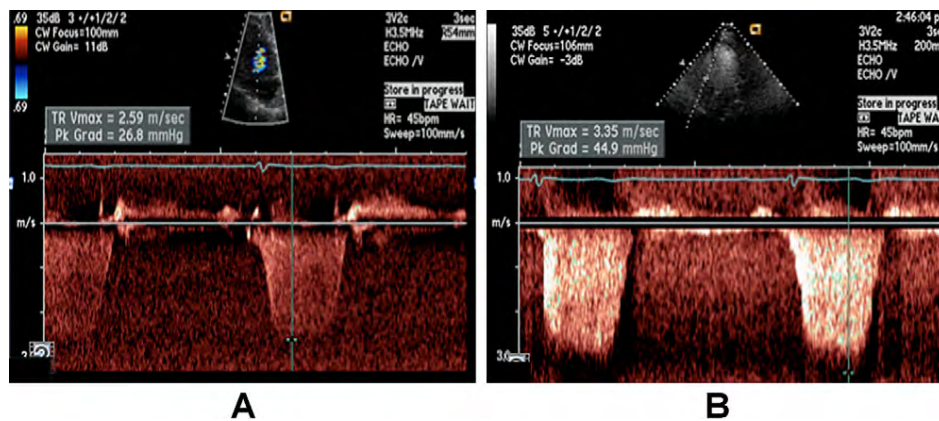


**Figure 12** (A) Tricuspid regurgitation signal that is not contrast enhanced and correctly measured at the peak velocity. (B) After contrast enhancement, the clear envelope has been obscured by noise, and the reader erroneously estimated a gradient several points higher. As this example shows, it is critical that only well-defined borders be used for velocity measurement, as slight errors are magnified by the second-order relationship between velocity and derived pressure.

this relationship, particularly at higher PA pressures.<sup>79,80</sup> In patients with very severe TR, the Doppler envelope may be cut off because of an early equalization of RV and RA pressures, and the simplified Bernoulli equation may underestimate the RV-RA gradient.

#### B. PA Diastolic Pressure

PADP can be estimated from the velocity of the end-diastolic pulmonary regurgitant jet using the modified Bernoulli equation:  $\text{PADP} = 4 \times (\text{end-diastolic pulmonary regurgitant velocity})^2 + \text{RA pressure}$ .

#### C. Mean PA Pressure

Once systolic and diastolic pressures are known, mean pressure may be estimated by the standard formula  $\text{mean PA pressure} = 1/3(\text{SPAP}) + 2/3(\text{PADP})$ . Mean PA pressure may also be estimated by using pulmonary AT measured by pulsed Doppler of the pulmonary artery in systole, whereby  $\text{mean PA pressure} = 79 - (0.45 \times \text{AT})$ .<sup>81</sup> The same group also found that in patients with ATs < 120 ms, the formula for mean PA pressure is  $90 - (0.62 \times \text{AT})$  performed better.<sup>82</sup> Generally, the shorter the AT (measured from the onset of the Q wave on electrocardiography to the onset of peak pulmonary flow velocity), the higher the PVR and hence the PA pressure, provided the heart rate is in the normal range of 60 to <100 beats/mins. The mean PA pressure can also be estimated as  $4 \times (\text{early PR velocity})^2 + \text{estimated RA pressure}$ .<sup>83</sup> An additional recently described method adds estimated RA pressure to the velocity-time integral of the TR jet to calculate a mean systolic pressure. This method has been validated by right heart catheterization and provides a value closer to one derived hemodynamically than the empirical methods.<sup>84,85</sup> Whenever possible, it is helpful to use several methods to calculate mean pressure so that the internal consistency of the data can be challenged and confirmed.

**Recommendations: Pulmonary hemodynamics are feasible in a majority of subjects using a variety of validated methods.<sup>86</sup> SPAP should be estimated and reported in all subjects with reliable tricuspid regurgitant jets. The recommended method is by TR velocity, using the simplified Bernoulli equation, adding an estimate of RA pressure as detailed above. In patients with PA hypertension or heart**

**failure, an estimate of PADP from either the mean gradient of the TR jet or from the pulmonary regurgitant jet should be reported. If the estimated SPAP is >35 to 40 mm Hg, stronger scrutiny may be warranted to determine if PH is present, factoring in other clinical information.**

#### D. Pulmonary Vascular Resistance

An elevation in SPAP does not always imply an increased PVR, as can be seen from the relationship whereby  $\Delta\text{pressure} = \text{flow} \times \text{resistance}$ . PVR distinguishes elevated pulmonary pressure due to high flow from that due to pulmonary vascular disease. PVR plays an important role in patients with heart failure with regard to transplantation eligibility. PVR can be estimated using a simple ratio of peak TR velocity (in meters per second) to the RVOT velocity-time integral (in centimeters).<sup>87-89</sup> This relationship is not reliable in patients with very high PVR, with measured PVR > 8 Wood units, as determined by invasive hemodynamic measurement.<sup>90</sup> One of the methods to determine PVR is illustrated in Figure 14.

A normal invasively measured PVR is <1.5 Wood units (120 dynes  $\cdot \text{cm/s}^2$ ), and for the purpose of clinical studies in PH, significant PH is defined as a PVR > 3 Wood units (240 dynes  $\cdot \text{cm/s}^2$ ).

**Recommendation: The estimation of PVR is not adequately established to be recommended for routine use but may be considered in subjects in whom pulmonary systolic pressure may be exaggerated by high stroke volume or misleadingly low (despite increased PVR) by reduced stroke volume. The noninvasive estimation of PVR should not be used as a substitute for the invasive evaluation of PVR when this value is important to guide therapy.**

#### E. Measurement of PA Pressure During Exercise

In normal subjects, exercise increases the stroke volume while the PVR decreases. Normal values are defined by SPAP < 43 mm Hg during exercise.<sup>91</sup> In well-trained athletes or those aged >55 years, SPAP as high as 55 to 60 mm Hg at peak exercise is encountered.<sup>92</sup> A pulmonary hypertensive response during exercise can be clinically important in several conditions, including valvular heart disease, heart failure,<sup>93</sup> and PH.<sup>94,95</sup> From the pathophysiologic viewpoint, on the



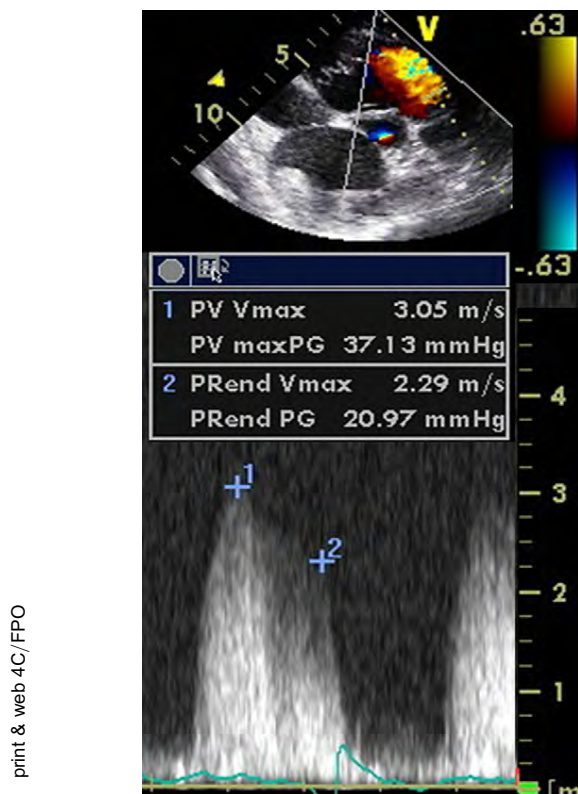


**Figure 13** Doppler echocardiographic determination of pulmonary artery (PA) diastolic pressure (PADP) and mean PA pressure by continuous-wave Doppler signal of pulmonic regurgitation. Point 1 denotes the maximal PI velocity at the beginning of diastole. Mean PA pressure correlates with  $4 \times (\text{early PI velocity})^2 + \text{estimated RAP}$ , in this example 37 mm Hg + RAP. Point 2 marks the PI velocity at end-diastole. PADP is correlated with  $4 \times (\text{end PI velocity})^2 + \text{estimated RAP}$ . In this example, PADP is 21 mm Hg + RAP.

basis of the fundamental equation of flow ( $F = \Delta P/R$ ), the abnormal exercise-induced increase in pressure can be ascribed to supranormal cardiac output (eg, in athletes) or to a normal increase in flow but a rise in resistance due to limited capability of the pulmonary vascular bed (eg, in chronic obstructive pulmonary disease or congenital heart disease). In this setting, the ratio of  $\Delta$ pressure (estimated by TR velocity) to flow (estimated by the RVOT time-velocity integral) may be helpful to distinguish whether the increased pressure is related to an increase in flow or in resistance.<sup>96</sup>

**Recommendation:** In patients with dyspnea of unknown etiology, with normal resting echocardiographic results and no evidence of coronary artery disease, it is reasonable to perform stress echocardiography to assess stress-induced PH. This technique should be considered as well in subjects with conditions associated with PA hypertension. Supine bicycle exercise is the preferred method for SPAP measurement. An upper limit of 43 mm Hg should be used in patients at nonextreme workloads. In subjects with valvular heart disease, the American College of Cardiology and American Heart Association cutoffs should be used to help guide management.

## NONVOLUMETRIC ASSESSMENT OF RIGHT VENTRICULAR FUNCTION

Determination of RV systolic function is similar to that of the left ventricle, albeit more challenging. The right ventricle has superficial circumferential muscle fibers responsible for its inward bellows movement, as well as inner longitudinal fibers that result in the base-to-apex contraction.<sup>20</sup> Compared with the left ventricle, the base-to-apex shortening assumes a greater role in RV emptying.

Global assessment of RV function includes the myocardial performance index (MPI), RV  $dP/dt$ , RV EF, and FAC (see above). Regional approaches include tissue Doppler–derived and 2D strain, Doppler-derived systolic velocities of the annulus ( $S'$ ), and TAPSE. Each method is affected by the same limitations from the corresponding left-sided techniques. The RV EF may not represent RV contractility in the setting of significant TR, just as the LV EF is limited by mitral regurgitation. For  $S'$  and TAPSE, the regional velocities or displacement of the myocardium in a single segment may not truly represent the function of the entire right ventricle. Regional strain measurements are plagued by the same issues, as well as that of poor reproducibility. There is a lack of outcomes data relating to quantification of RV systolic function. Nonetheless, each of the methods is described below, reference values are displayed, and recommendations for measurements are proposed.

### A. Global Assessment of RV Systolic Function

**RV  $dP/dt$ .** The rate of pressure rise in the ventricles ( $dP/dt$ ) is an invasive measurement developed and validated as an index of ventricular contractility or systolic function. It was initially described by Gleason and Braunwald<sup>97</sup> in 1962 in both the left and right ventricles.

Although less studied and more sparsely used than for the left ventricle, RV  $dP/dt$  can also be accurately estimated from the ascending limb of the TR continuous-wave Doppler signal.<sup>98,99</sup> RV  $dP/dt$  is commonly calculated by measuring the time required for the TR jet to increase in velocity from 1 to 2 m/s. Using the simplified Bernoulli equation, this represents a 12 mm Hg increase in pressure. The  $dP/dt$  is therefore calculated as 12 mm Hg divided by this time (in seconds), yielding a value in millimeters of mercury per second. Although the time from 1 to 2 m/s is most commonly used, the best correlation between echocardiographic and invasive measures was found by using the time for the TR velocity to increase from 0.5 to 2 m/s.<sup>99</sup> In this case, the numerator for the calculation is 15 mm Hg, representing the pressure difference as calculated from the simplified Bernoulli equation between 2 and 0.5 m/s.

**Advantages:** This is a simple technique with a sound physiologic basis.

**Disadvantages:** There are limited data in both normal subjects and pathologic conditions. RV  $dP/dt$  is load dependent. RV $dP/dt$  will be less accurate in severe TR because of neglect of the inertial component of the Bernoulli equation and the rise in RA pressure.

**Recommendations:** Because of the lack of data in normal subjects, RV  $dP/dt$  cannot be recommended for routine uses. It can be considered in subjects with suspected RV dysfunction. RV  $dP/dt < \text{approximately } 400 \text{ mm Hg/s}$  is likely abnormal.

**RIMP.** The MPI, also known as the RIMP or Tei index, is a global estimate of both systolic and diastolic function of the right ventricle. It is based on the relationship between ejection and nonejection work of



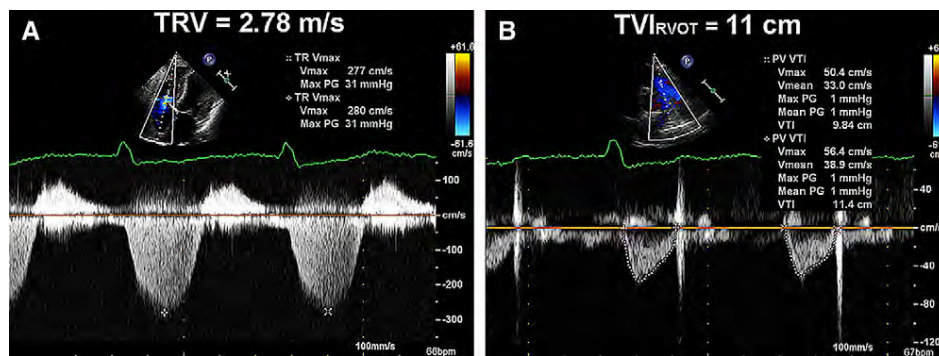


**Figure 14** The two elements needed to calculate the noninvasive index of pulmonary vascular resistance (PVR) are found in this example. The ratio of peak tricuspid regurgitant velocity (TRV) (2.78 m/s) to the time-velocity integral (TVI) (11 cm) in the right ventricular outflow tract (RVOT) is abnormal at 0.25 (normal,  $\leq 0.15$ ). The estimated PVR is 2.68 using the formula  $(\text{TRVmax}/\text{RVOT TVI}) \times 10 + 0.16$ .<sup>84</sup> Adapted with permission from *J Am Soc Echocardiogr*.<sup>52</sup>

the heart. The MPI is defined as the ratio of isovolumic time divided by ET, or  $[(\text{IVRT} + \text{IVCT})/\text{ET}]$  (Figure 16).

The measure remains accurate within a broad range of heart rates,<sup>100</sup> though the components should be measured with a constant R-R interval to minimize error. Although the MPI was initially thought to be relatively independent of preload, this has been questioned in more recent studies. In addition, the MPI has been demonstrated to be unreliable when RA pressure is elevated (eg, RV infarction), as there is a more rapid equilibration of pressures between the RV and RA, shortening the IVRT and resulting in an inappropriately small MPI.<sup>101</sup>

The right-sided MPI can be obtained by two methods: the pulsed Doppler method and the tissue Doppler method. In the pulsed Doppler method, the ET is measured with pulsed Doppler of RV outflow (time from the onset to the cessation of flow), and the tricuspid (valve) closure-opening time is measured with either pulsed Doppler of the tricuspid inflow (time from the end of the transtricuspid A wave to the beginning of the transtricuspid E wave) or continuous Doppler of the TR jet (time from the onset to the cessation of the jet). These measurements are taken from different images, and one must therefore attempt to use beats with similar R-R intervals to obtain a more accurate RIMP value. In the tissue Doppler method, all time intervals are measured from a single beat by pulsing the tricuspid annulus (shown below). As was demonstrated for the LV MPI,<sup>102,103</sup> it is important to note that the correlation between both methods is modest and that normal values differ on the basis of the method chosen.

The MPI has prognostic value in patients with PH at a single point in time,<sup>100</sup> and changes in MPI correlate with change in clinical status in this patient group.<sup>104</sup> It has also been studied in RV infarction, hypertrophic cardiomyopathy, and congenital heart disease, among others.<sup>105-110</sup> The MPI has been measured in healthy individuals and in normal control subjects in 23 studies with >1000 subjects. The upper reference limit is 0.40 by pulsed Doppler and 0.55 by tissue Doppler (Table 4).

**Advantages:** This approach is feasible in a large majority of subjects both with and without TR, the MPI is reproducible, and it avoids the geometric assumptions and limitations of complex RV geometry. The pulsed tissue Doppler method allows for measurement of MPI as well as  $S'$ ,  $E'$ , and  $A'$ , all from a single image.

**Disadvantages:** The MPI is unreliable when RV ET and TR time are measured with differing R-R intervals, as in atrial fibrillation.

Moreover, it is load dependent and unreliable when RA pressure is elevated.

**Recommendations:** The MPI may be used for initial and serial measurements as an estimate of RV function in complement with other quantitative and nonquantitative measures. The upper reference limit for the right-sided MPI is 0.40 using the pulsed Doppler method and 0.55 using the pulsed tissue Doppler method. It should not be used as the sole quantitative method for evaluation of RV function and should not be used with irregular heart rates.

#### B. Regional Assessment of RV Systolic Function

**TAPSE or Tricuspid Annular Motion (TAM).** The systolic movement of the base of the RV free wall provides one of the most visibly obvious movements on normal echocardiography. TAPSE or TAM is a method to measure the distance of systolic excursion of the RV annular segment along its longitudinal plane, from a standard apical 4-chamber window. TAPSE or TAM represents longitudinal function of the right ventricle in the same way as mitral annular plane systolic excursion by Doppler tissue imaging does with the left ventricle. It is inferred that the greater the descent of the base in systole, the better the RV systolic function. As with other regional methods, it assumes that the displacement of the basal and adjacent segments in the apical 4-chamber view is representative of the function of the entire right ventricle, an assumption that is not valid in many disease states or when there are regional RV wall motion abnormalities. TAPSE is usually acquired by placing an M-mode cursor through the tricuspid annulus and measuring the amount of longitudinal motion of the annulus at peak systole (Figure 17).

In the initial validation study by Kaul et al,<sup>111</sup> TAPSE correlated strongly with radionuclide angiography, with low interobserver variability. It has also been validated against biplane Simpson RV EF and RV fractional area shortening.<sup>112,113</sup> In a study of 750 patients with a variety of cardiac conditions, compared with 150 age-matched normal controls, a TAPSE cutoff value  $< 17$  mm yielded high specificity, though low sensitivity to distinguish abnormal from normal subjects.<sup>114</sup> In total, there have been >40 studies with >2000 normal subjects evaluating the utility of TAPSE or TAM (Table 4).

**Advantages:** TAPSE is simple, less dependent on optimal image quality, and reproducible, and it does not require sophisticated equipment or prolonged image analysis.

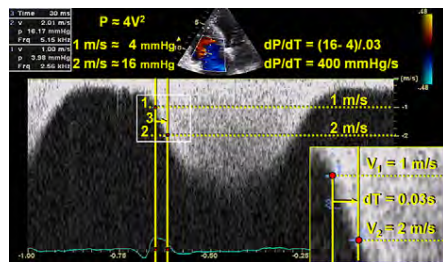


**Figure 15** Point 1 represents the point at which the tricuspid regurgitation (TR) signal meets the 1 m/s velocity scale marker, while point 2 represents the point at which the TR signal meets the 2 m/s velocity scale marker. Point 3 represents the time required for the TR jet to increase from 1 to 2 m/s. In this example, this time is 30 ms, or 0.03 seconds. The  $dP/dt$  is therefore 12 mm Hg/0.03 seconds, or 400 mm Hg/s.

**Disadvantages:** TAPSE assumes that the displacement of a single segment represents the function of a complex 3D structure. Furthermore, it is angle dependent, and there are no large-scale validation studies. Finally, TAPSE may be load dependent.

**Recommendations:** TAPSE should be used routinely as a simple method of estimating RV function, with a lower reference value for impaired RV systolic function of 16 mm.

**Doppler Tissue Imaging.** Among the most reliably and reproducibly imaged regions of the right ventricle are the tricuspid annulus and the basal free wall segment. These regions can be assessed by pulsed tissue Doppler and color-coded tissue Doppler to measure the longitudinal velocity of excursion. This velocity has been termed the RV  $S'$  or systolic excursion velocity. To perform this measure, an apical 4-chamber window is used with a tissue Doppler mode region of interest highlighting the RV free wall. The pulsed Doppler sample volume is placed in either the tricuspid annulus or the middle of the basal segment of the RV free wall (Figure 18). Because this technique uses Doppler, care must be taken to ensure optimal image orientation to avoid the underestimation of velocities. Alternatively, color-coded tissue Doppler is acquired at high frame rates and analyzed offline, by placing a region of interest in the segment to be interrogated. Platform-specific software then generates velocity profiles over the cardiac cycle. The velocity  $S'$  is read as the highest systolic velocity, without overgaining the Doppler envelope. Assessment of the mid and apical ventricular free wall velocities is discouraged in the routine echocardiographic studies, because there is a lower rate of obtaining adequate signals<sup>115</sup> and greater variability. Because the interventricular septum does not exclusively reflect RV function, it should not be used alone to assess the right ventricle.

A number of validation studies have been performed comparing pulsed tissue Doppler velocities of the tricuspid annulus with radionuclide angiography, showing good correlations and good discriminative ability between normal and abnormal RV EFs.

$S'$  has one of the few population-based validation studies for the right ventricle. The Umeå General Population Heart Study in Sweden assessed RV regional function in 235 healthy individuals aged 20 to 90 years.<sup>115</sup> Mean values in normal populations are approximately 15 cm/s at the annulus and basal segment of the RV free wall, with lower velocities at the mid and apical segments. When 43 studies were pooled with >2000 normal controls, a lower reference limit of normal controls was 10 cm/s.

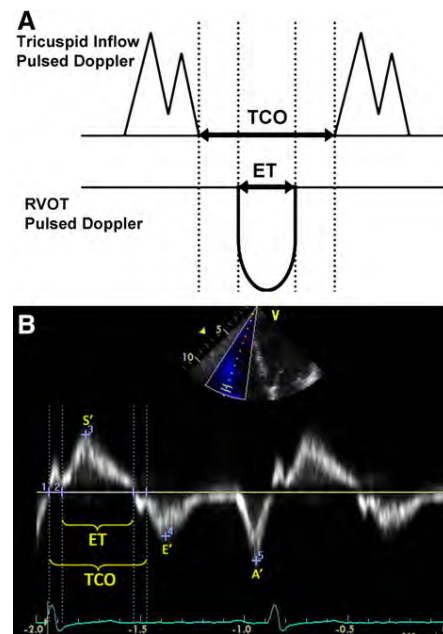


**Figure 16** Calculation of right ventricular myocardial performance index (MPI) by pulsed Doppler (A) and pulsed tissue Doppler (B). The tricuspid (valve) closure opening time (TCO) encompasses isovolumic contraction time, ejection time (ET), and isovolumic relaxation time. In the pulsed Doppler method, TCO can also be measured by the duration of the tricuspid regurgitation continuous-wave Doppler signal.  $MPI = (TCO - ET)/ET$ . Note that  $S'$ ,  $E'$ , and  $A'$  are also measured from the same pulsed Doppler tissue image.

Color-coded tissue Doppler yields lower velocities, because the encoded data represent mean velocities. Color-coded tissue Doppler studies have been performed in healthy volunteers and normal controls. Mean annular velocities average 8.5 to 10 cm/s, while basal RV free wall velocities are slightly higher at 9.3 to 11 cm/s. Two studies have demonstrated slightly lower velocities in older groups of subjects.<sup>116,117</sup> Mid and distal segments were less reliably acquired, with greater variability. The reference limit pooled from the available studies is 6 cm/s but with slightly broader 95% confidence intervals around this reference limit (Table 4).

**Advantages:** A simple, reproducible technique with good discriminatory ability to detect normal versus abnormal RV function, pulsed Doppler is available on all modern ultrasound equipment and does not require additional software. In addition, color-coded Doppler-derived  $S'$  may be obtained and analyzed offline on certain platforms.

**Disadvantages:** This technique is less reproducible for nonbasal segments and is angle dependent, and there are limited normative data in all ranges and in both sexes. Moreover, it assumes that the function of a single segment represents the function of the entire right ventricle, which is not likely in conditions that include regionality, such as RV infarction or pulmonary embolism.

**Recommendations:** Interrogation of  $S'$  by pulsed tissue Doppler is a simple and reproducible measure to assess basal RV free wall function and should be used in the assessment of RV function.  $S' < 10$  cm/s should raise the suspicion for abnormal RV function, particularly in a younger adult

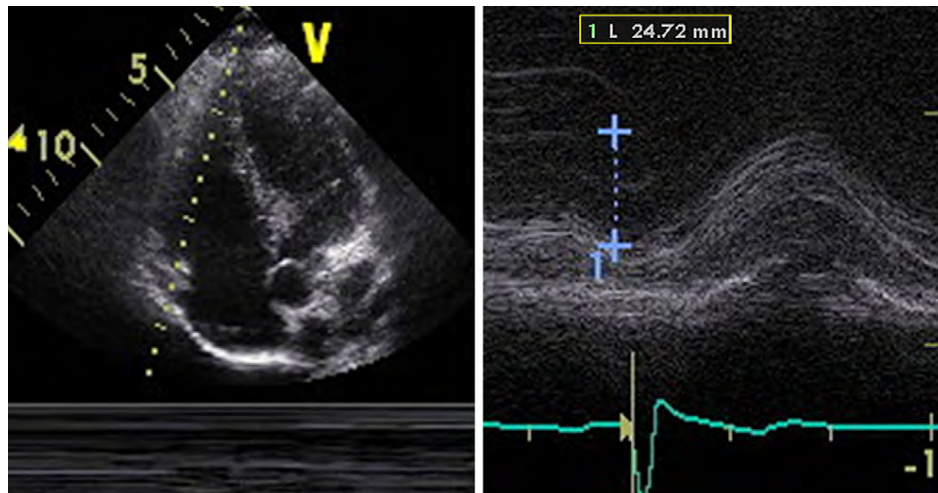


**Figure 17** Measurement of tricuspid annular plane systolic excursion (TAPSE).

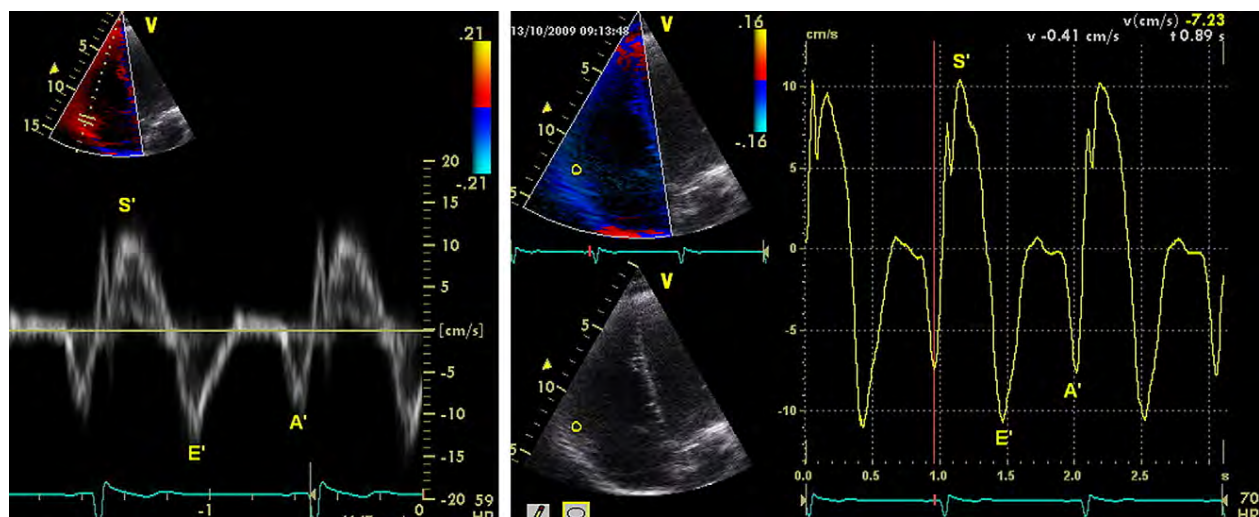


**Figure 18** Tissue Doppler of the tricuspid annulus in a patient with normal right ventricular systolic function: (left) pulsed and (right) color-coded offline analysis.

**patient. There are insufficient data in the elderly. Offline analysis by color-coded tissue Doppler currently remains a research tool, with less data and wider confidence intervals for normal values.**

#### **Myocardial Acceleration During Isovolumic Contraction.**

Myocardial acceleration during isovolumic contraction is defined as the peak isovolumic myocardial velocity divided by time to peak velocity and is typically measured for the right ventricle by Doppler tissue imaging at the lateral tricuspid annulus (Figure 19). For the calculation of IVA, the onset of myocardial acceleration is at the zero crossing point of myocardial velocity during isovolumic contraction. Isovolumic acceleration (IVA) appears to be less load dependent than ejection period indices under a variety of physiologic conditions.<sup>118-121</sup>

In a series of cardiac patients under anesthesia, RV IVA appeared to be the most consistent tissue Doppler variable for the evaluation of RV function measured by either transthoracic echocardiography (lat-

eral wall) or transesophageal echocardiography (inferior wall).<sup>122</sup> RV IVA has been demonstrated to correlate with the severity of illness in conditions affecting right heart function, including obstructive sleep apnea,<sup>123</sup> mitral stenosis,<sup>124,125</sup> repaired tetralogy of Fallot with pulmonary regurgitation,<sup>126</sup> and transposition of the great arteries following an atrial switch procedure.<sup>127</sup>

Normal RV IVA values have been obtained from studies that have included a control group of normal adults and/or children. It appears to be age dependent, with the highest values found between the ages of 10 and 20 years.<sup>128</sup> As with all tissue Doppler indices, the acquisition technique is important to document. Pulsed-wave tissue Doppler values are up to 20% higher than color-coded tissue Doppler values.<sup>116</sup> In addition, IVA has been shown to vary with heart rate,<sup>121</sup> and indexing to heart rate may be appropriate in some clinical situations. The lower reference limit by pulsed-wave Doppler tissue imaging, pooled from 10 studies, is 2.2 m/s<sup>2</sup>, with a broad 95% confidence interval of 1.4 to 3.0 (Table 4).



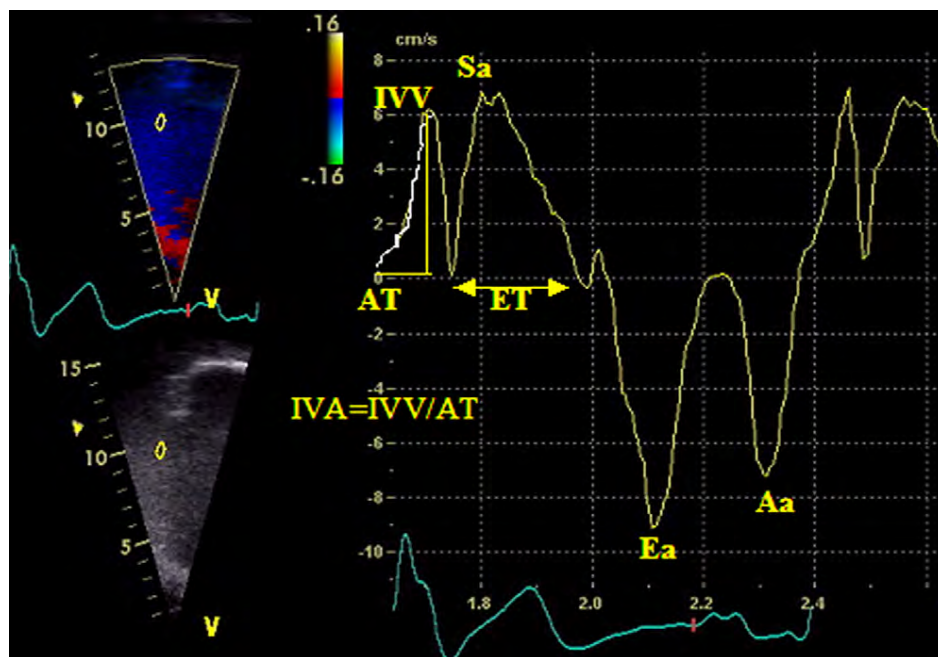


**Figure 19** Doppler tissue velocities and time intervals obtained at lateral tricuspid valve annulus. Aa, Peak velocity during atrial contraction; AT, acceleration time; Ea, peak velocity during early diastole; ET, ejection time; IVA, myocardial acceleration during isovolumic contraction; IVV, peak myocardial velocity during isovolumic contraction; Sa, peak velocity during ejection period of systole. Reproduced with permission from *J Am Soc Echocardiogr*.<sup>182</sup>

**Advantages:** RV IVA is a relatively load independent measurement of global RV systolic function that has been shown to correlate with severity of illness in conditions affecting right heart function.

**Disadvantages:** There are limited normative data available, and RV IVA is an angle-dependent Doppler measurement that appears to vary with age and heart rate.

**Recommendations:** In studies in patients with conditions affected by RV function, RV IVA may be used, and when used, it should be measured at the lateral tricuspid annulus. RV IVA is not recommended as a screening parameter for RV systolic function in the general echocardiography laboratory population. Because of the broad confidence interval around its lower reference limit, no reference value can be recommended.

**Regional RV Strain and Strain Rate.** Strain is defined as percentage change in myocardial deformation, while its derivative, strain rate, represents the rate of deformation of myocardium over time. Strain rate has been closely correlated with myocardial contractility in in vitro and in vivo experimental settings.<sup>129</sup>

One-dimensional strain is acquired using Doppler tissue imaging and is consequentially angle dependent. It is most reproducible in the apical 4-chamber view, interrogating the basal, mid, and, to a lesser degree, apical segments of the RV free wall. As a result, one is limited to mostly longitudinal strain. A number of algorithms have been adapted to try to deal with issues in signal to noise ratio, and varying groups studying strain and strain rate in myocardial performance have used different protocols. As a result, values obtained may not be the same across ultrasound platforms, further increasing difficulties in reproducibility.

To calculate strain, high frame rates are required, ideally  $\geq 150$  frames/s. As such, a narrow imaging sector focusing on the RV

free wall is desired. Care should be taken to align the segment in the center of the sector to avoid errors due to the angle dependence of Doppler. A maximum tolerance of  $10^\circ$  to  $15^\circ$  off the axis of contraction is recommended.<sup>130</sup> Imaging is in color-coded tissue Doppler mode, and  $\geq 3$  beats are acquired with suspended respiration. Values for strain and SR are then derived offline on the system or workstation using equipment-specific algorithms by placing sample volume(s) or regions of interest of varying sizes in the mid portion of the segment(s).

Strain and strain rate values have been studied in a number of conditions affecting the right heart, including arrhythmogenic RV dysplasia,<sup>131</sup> pulmonary embolism,<sup>132</sup> PH,<sup>133</sup> systemic right ventricle,<sup>134</sup> and amyloidosis.<sup>135-137</sup> There is a lack of normative data for strain and strain rate measures of the right ventricle, and most values in normal subjects represent small groups of patients representing control arms in pathologic studies. Values for basal, mid, and apical free wall segments of the right ventricle are displayed in Table 5. Pooled data yield results with very large SDs around the mean values. As such, lower reference values based on 95% confidence intervals are not clinically useful.

**Advantages:** Regional RV strain represents a potential means to assess myocardial contractility that is less load dependent, and may be applicable across a wide range of pathologies.

**Disadvantages:** There is a lack of normative data. In addition, this measure is angle dependent and has a poor signal-to-noise ratio. Finally, this is a complex measure with a high degree of variability that requires additional software and offline analysis.

**Recommendations:** The significant disadvantages listed above limit the clinical use of regional RV strain. Reference limits cannot be recommended, because of very wide confidence intervals both around the mean values and around the reference limits. Strain and strain rate



**Table 5** Longitudinal strain and strain rate

Variable	Studies	n	LRV (95% CI)	Mean (95% CI)	URV (95% CI)
2D peak strain rate at the base ( $s^{-1}$ )	1	61	0.70 (0.50-0.90)	1.62 (1.50-1.74)	2.54 (2.34-2.74)
2D peak strain rate at the mid cavity ( $s^{-1}$ )	2	80	0.85 (0.66-1.04)	1.54 (1.46-1.62)	2.23 (2.04-2.42)
2D peak strain rate at the apex ( $s^{-1}$ )	2	80	0.86 (0.46-1.25)	1.62 (1.46-1.79)	2.39 (1.99-2.78)
2D peak strain at the base (%)	5	183	18 (14-22)	28 (25-32)	39 (35-43)
2D peak strain at the mid cavity (%)	4	125	20 (15-24)	29 (25-33)	38 (34-43)
2D peak strain at the apex (%)	4	145	19 (15-22)	29 (26-32)	39 (36-43)
Doppler peak strain rate at the base ( $s^{-1}$ )	7	261	1.00 (0.63-1.38)	1.83 (1.50-2.15)	2.66 (2.28-3.03)
Doppler peak strain rate at the mid cavity ( $s^{-1}$ )	5	187	0.98 (0.68-1.28)	1.88 (1.73-2.03)	2.79 (2.49-3.09)
Doppler peak strain rate at the apex ( $s^{-1}$ )	5	204	1.14 (0.60-1.69)	2.04 (1.57-2.51)	2.93 (2.39-3.48)
Doppler peak strain at the apex (%)	7	290	17 (12-21)	30 (27-34)	44 (39-48)
Doppler peak strain at the base (%)	11	385	13 (9-17)	29 (27-31)	45 (41-49)
Doppler peak strain at the mid cavity (%)	7	269	13 (9-18)	31 (29-32)	48 (44-52)

CI, Confidence interval; LRV, lower reference value; 2D, two-dimensional; URV, upper reference value.

### remain research tools in experienced labs until their limitations can be overcome.

**Two-Dimensional Strain.** Strain measurement has been possible using 2D images, resulting in the estimation of 2D strain. This new measure of regional and global contractility uses frame-by-frame tracking of unique speckles in the myocardium with an algorithm that allows tracking the speckle location on sequential images using correlation criteria and sum of absolute differences. In one ultrasound platform, this process is performed using velocity vector tracking. In addition to generating strain curves in individual segments, algorithms exist to average strain over the entire chamber. A significant advantage of 2D tracking methods is that they are not angle dependent within the acquired imaging plane, but proper alignment of image planes is still important. Two-dimensional strain has been applied and validated in the LV and has recently been studied to assess RV function in systemic right ventricle and in patients with PH.<sup>134</sup>

**Advantages:** This technique is relatively angle independent and possesses an improved signal-to-noise ratio. It can also provide regional function estimates, as well as a more “global” function.

**Disadvantages:** There is a lack of normative data regarding this technique, which also requires additional validation. Requiring additional software, it is dependent on adequate image quality. The “global” nature is derived only from a single view, making it not a truly global assessment of RV function. Finally, different algorithms in different platforms may result in different normal ranges.

**Recommendations: Because of the lack of reproducibility and the paucity of data, this technique is not recommended for routine clinical use. No reference limits can be recommended, because of the large degree of variability.**

### SUMMARY OF RECOMMENDATIONS FOR THE ASSESSMENT OF RIGHT VENTRICULAR SYSTOLIC FUNCTION

Visual assessment of RV systolic function gives the reader an initial qualitative evaluation of RV systolic function but remains insufficient in this era of standardization. There are several simple and reproducible methods of assessing RV systolic function that should be incorporated into the routine echocardiographic assessment. These are FAC,

TAPSE, pulsed tissue Doppler  $S'$ , and MPI. Combining more than one measure of RV function, such as  $S'$  and MPI, may more reliably distinguish normal from abnormal function.<sup>113</sup> It is strongly recommended that at least one of the above quantitative measures be incorporated into the routine echocardiographic examination and report, and this is particularly important when RV dysfunction is suspected and/or when the clinical indication for the study relates to a condition that may affect the right ventricle. More sophisticated techniques such as IVA, strain, and strain rate are not currently recommended as routine and are best reserved for specific clinical and research applications in experienced laboratories.

### RIGHT VENTRICULAR DIASTOLIC FUNCTION

#### A. RV Diastolic Dysfunction

The right ventricle is more than a passive chamber. Acute injury to the right ventricle, most notably in the context of RV myocardial infarction, results in marked diastolic dysfunction with elevated filling pressures and clinically apparent jugular venous distension.<sup>138-140</sup> Pathophysiology of RV diastolic dysfunction is much more complex than simply measuring the thickness of the myocardium.<sup>141-145</sup> A growing number of acute and chronic conditions have been associated with RV diastolic dysfunction, including both pressure and volume overload pathologies, primary lung disease, ischemic heart disease, congenital heart disease, cardiomyopathies, LV dysfunction (via ventricular interdependence), systemic diseases, and the physiologic aging process (Table 7).

#### B. Measurement of RV Diastolic Function

From the apical 4-chamber view, the Doppler beam should be aligned parallel to the RV inflow. Proper alignment may be facilitated by displacing the transducer medially toward the lower parasternal region. The sample volume should be placed at the tips of the tricuspid leaflets.<sup>141</sup> With this technique, measurement of transtricuspid flow velocities can be achieved in most patients, with low interobserver and intraobserver variability.<sup>146</sup> Care must be taken to measure at held end-expiration and/or take the average of  $\geq 5$  consecutive beats.<sup>147</sup> The presence of moderate to severe TR or atrial fibrillation could confound diastolic parameters, and most studies excluded such patients.

**Table 6** Diastolic function

Variable	Studies	n	LRV (95% CI)	Mean (95% CI)	URV (95% CI)
E (cm/s)	55	2866	35 (33-37)	54 (52-56)	73 (71-75)
A (cm/s)	55	3096	21 (19-24)	40 (38-41)	58 (55-60)
E/A ratio*	56	2994	0.8 (0.7-0.9)	1.4 (1.4-1.5)	2.1 (2.0-2.2)
Deceleration time (ms)	25	1284	120 (105-134)	174 (163-186)	229 (214-243)
IVRT (ms)	23	1241	23 (16-30)	48 (43-53)	73 (66-80)
E' (cm/s)	40	1688	8 (7-9)	14 (13-14)	20 (19-21)
A' (cm/s)	37	1575	7 (6-8)	13 (12-14)	20 (19-21)
E'/A' ratio	29	1053	0.5 (0.4-0.6)	1.2 (1.1-1.3)	1.9 (1.7-2.0)
E/E' ratio	3	359	2 (1-2)	4 (4-4)	6 (5-7)

CI, Confidence interval; IVRT, Isovolumic relaxation time; LRV, lower reference value; URV, upper reference value.

\*Age-dependent: average E/A ratio = 1.6 in the third decade of life, decreasing by 0.1 for every subsequent decade.

Estimation of RA pressure by measurement of IVC diameter and collapse with inspiration as described above should be factored into the determination of RV diastolic function. The parameters used to assess RV diastolic function are essentially the same as those used to assess the left side. Those that have been most validated are Doppler velocities of the transtricuspid flow (E, A, and E/A), tissue Doppler velocities of the tricuspid annulus (E', A', E'/A'), deceleration time, and IVRT (Table 6). The tricuspid E/E' ratio, RA area or volume, and diastolic strain rate appear promising and have attracted interest in recent studies. In addition, the presence of late diastolic antegrade flow in the pulmonary artery (measured by pulsed Doppler with the sample volume positioned midway between the pulmonary valve leaflets and the pulmonary artery bifurcation) is a sign of restrictive diastolic filling.<sup>148</sup> This sign, mainly described after tetralogy of Fallot repair, occurs when the elevated RV end-diastolic pressure causes premature opening of the pulmonary valve and transmission of the RA contraction A wave in the pulmonary artery.

#### C. Effects of Age, Respiration, Heart Rate, and Loading Conditions

Most studies have shown that there is a modest correlation ( $r \approx 0.30$ ) between the E/A ratio and increasing age. The E/A ratio decreases by approximately 0.1 per decade.<sup>117,141,149,150</sup> Inspiration causes an increase in E and therefore an increase in the E/A ratio. Tachycardia causes an increase in E but a relatively greater increase in A and therefore a decrease in the E/A ratio.<sup>141,150,151</sup> When comparing Doppler parameters between patients or in the same patient, one must consider the effect of these hemodynamic variables on the observed parameters. Because of its thin wall, the right ventricle is very sensitive to afterload (wall stress), especially in the presence of RV myocardial disease such as ischemia or infarction.<sup>144,152,153</sup> It is also sensitive to changes in preload, whereby a reduction in preload causes a decrease in E but a relatively smaller decrease in A and therefore a decrease in E/A.<sup>154-156</sup> Tissue Doppler is less load dependent, because a reduction in preload causes an equal decrease in E' and A' and therefore an unchanged E'/A' ratio. Importantly, tissue Doppler should be used to differentiate normal from pseudonormal filling patterns with elevated filling pressures as are hepatic vein flow patterns and vena cava size and collapse.<sup>15</sup> Last, the physiologic response to exercise is to increase both early rapid filling and atrial contribution. In ischemic patients, the pathophysiologic response is a failure of the early rapid filling to increase and a heightened dependency on atrial contribution and consequent elevated RA pressure.<sup>157</sup>

#### D. Clinical Relevance

A small number of studies have evaluated the clinical impact of RV diastolic dysfunction. The tricuspid E/E' ratio and RA volume have been shown to correlate well with hemodynamic parameters. An E/E' ratio  $\geq 4$  had high sensitivity and specificity for predicting RA pressure  $\geq 10$  mm Hg in non-cardiac surgery intensive care unit patients,<sup>158</sup> while an E/E' ratio  $> 8$  had good sensitivity and specificity for predicting RA pressure  $\geq 10$  mm Hg in cardiac transplantation patients.<sup>159</sup> In patients with chronic heart failure and PH, the presence of RV diastolic dysfunction was associated with worse functional class and was an independent predictor of mortality.<sup>100,160</sup> Diastolic filling patterns reflect response to therapy, improving with successful treatment of a variety of cardiac conditions.<sup>161-164</sup> Finally, RV diastolic dysfunction may be clinically useful because it serves as an early and more easily quantifiable marker of subclinical RV dysfunction. Multiple studies have shown that RV diastolic dysfunction is usually present before apparent systolic dysfunction and before RV dilatation or RVH.

**Recommendations: Measurement of RV diastolic function should be considered in patients with suspected RV impairment as a marker of early or subtle RV dysfunction, or in patients with known RV impairment as a marker of poor prognosis. Transtricuspid E/A ratio, E/E' ratio, and RA size have been most validated and are the preferred measures (Table 6). Grading of RV diastolic dysfunction should be done as follows: tricuspid E/A ratio  $< 0.8$  suggests impaired relaxation, a tricuspid E/A ratio of 0.8 to 2.1 with an E/E' ratio  $> 6$  or diastolic flow predominance in the hepatic veins suggests pseudonormal filling, and a tricuspid E/A ratio  $> 2.1$  with a deceleration time  $< 120$  ms suggests restrictive filling (as does late diastolic antegrade flow in the pulmonary artery). Further studies are warranted to validate the sensitivity and specificity and the prognostic implications of this classification.**

#### CLINICAL AND PROGNOSTIC SIGNIFICANCE OF RIGHT VENTRICULAR ASSESSMENT

Quantitative assessment of RV size and function has proven to be of important clinical value in a number of cardiac and pulmonary diseases. Numerous publications have demonstrated the prognostic significance of RV function.

**Table 7** Conditions associated with right ventricular diastolic dysfunction

Condition
• Pulmonary embolism
• Pulmonary arterial hypertension
• Smoking
• Chronic obstructive pulmonary disease
• Cystic fibrosis
• Acute hypoxia
• Myocardial infarction or ischemia due to (proximal) right coronary artery lesion
• Repaired tetralogy of Fallot
• Repaired transposition of the great arteries
• Chronic heart failure
• Cardiac transplantation
• Arrhythmogenic right ventricular cardiomyopathy
• Hypertrophic cardiomyopathy
• Chagas disease
• Essential hypertension
• Aortic stenosis
• Aortic regurgitation
• Mitral regurgitation
• Myocardial infarction due to left anterior descending coronary artery lesion
• Diabetes mellitus
• Hypothyroidism
• Amyloidosis
• Rheumatoid arthritis
• Systemic sclerosis
• Antiphospholipid antibody syndrome
• Bechet's vasculitis
• $\beta$ -thalassemia
• Renal transplantation
• Hepatopulmonary syndrome
• Normal neonates
• Aging

The normal right ventricle is accustomed to low pulmonary resistance and because of its thin walls is relatively compliant. Hence, conditions that acutely increase PVR, such as pulmonary embolism, result in increases in RV size prior to the augmentation of pulmonary pressures, which ultimately may result as the ventricle hypertrophies.<sup>165</sup> Dilatation of the right ventricle thus is the first marker of increases in PVR. As the right ventricle hypertrophies to overcome the elevated PVR, RV size, indicated by diameter or volumes, can decrease, and the RV free wall thickness increases with ultimate increase in RVSP. In patients with acute pulmonary embolism, initial increases in RV volume and diameters are often accompanied by a specific pattern of abnormal regional wall motion in which the mid RV free wall becomes dyskinetic with relative sparing of the base and apex.<sup>166</sup> These findings have important prognostic implications in patients with pulmonary embolism<sup>167</sup> and are entirely reversible with improvement in pulmonary hemodynamics.<sup>36</sup> In patients with longstanding pulmonary vascular disease or other forms of secondary PH (including from chronic obstructive pulmonary disease, emphysema, or other forms of pulmonary parenchymal disease), the right ventricle tends to hypertrophy and normalize volumes at first, followed by eventual and progressive dilatation.<sup>168</sup>

RV size and function can also be adversely affected by diseases intrinsic to the left ventricle. Patients with LV dysfunction secondary to myocardial infarction or heart failure are at increased risk for both RV dilatation and dysfunction.<sup>169-172</sup> Indeed, RV dysfunction is one of the most powerful independent predictors of outcome following myocardial infarction, even in the absence of overt RV infarction.<sup>37,38</sup> Similar findings have been shown in patients with chronic heart failure and in stable survivors a year after infarction.<sup>173</sup> Data from the Evaluation Study of Congestive Heart Failure and Pulmonary Artery Catheterization Effectiveness (ESCAPE) suggest that elevation in pulmonary pressures directly may contribute to alterations in RV size and function in patients with heart failure.<sup>174</sup> Moreover, sleep apnea in patients with heart failure may also contribute substantially to alterations in RV function and size.<sup>175</sup> These data suggest that clinical assessment of the right ventricle can add incrementally to the standard echocardiographic assessment in patients with left-sided heart disease.

RV size and function can also be affected by diseases affecting the tricuspid valve resulting in substantial TR. These include carcinoid disease,<sup>176,177</sup> in which the tricuspid leaflets can retract and become functionally incompetent; rheumatic tricuspid disease<sup>178</sup>; myxomatous degeneration of the tricuspid valve; or any other situation in which the tricuspid valve becomes incompetent. The volume overload that ensues with TR leads to dilatation of the right ventricle, which can itself result in further TR.

The most common congenital abnormality that affects the right ventricle in adult cardiology is atrial septal defect. The increased flow resulting from the shunt can lead to elevation in pulmonary pressures and RV dilatation. The population of patients with postoperative tetralogy of Fallot with severe pulmonary regurgitation presenting with severe RV dilatation and diminished function is increasing. Other congenital abnormalities, such as Ebstein anomaly, and more complex congenital disorders can affect the right ventricle. Situations in which RV morphology appears to be particularly unusual should raise the suspicion of more complex congenital heart disease.

## CONCLUSION

Echocardiographic assessment of the right ventricle has been largely qualitative, primarily because of the difficulty with assessing RV volumes because of its unusual shape.<sup>179,180</sup> Hence, there are minimal quantitative data overall on RV size and function in normal controls and in disease states. A gradual shift to more quantitative approaches for the assessment of RV size and function will help standardize assessment of the right ventricle across laboratories and allow clinicians to better incorporate assessment of the right heart into an echocardiographic evaluation. Improvements in 3D imaging will result in increased use and have the potential to help in the clinical assessment of RV size and function.<sup>181</sup>

This guidelines document provides clinicians basic views to assess the right ventricle and right atrium, the various parameters to assess RV systolic and diastolic function, and the normal reference values from pooled data. This will enable echocardiographers to distinguish an abnormal right ventricle from a normal one. It is hoped that this document will lead to further work in establishing normal ranges in larger populations and that the application of the values included will enhance the value of echocardiography in recognizing RV dysfunction in clinical practice, in improving disease detection and in patient follow-up.



## ACKNOWLEDGMENTS

The members of the writing group gratefully acknowledge the assistance of the members of the Guidelines and Standards Committee of the ASE for their careful review of the manuscript. We also thank Dr Russell Steele, PhD, for his assistance with statistical design and Renee Atallah, MSc, for her assistance in manuscript preparation.

## NOTICE AND DISCLAIMER

This report is made available by ASE as a courtesy reference source for its members. This report contains recommendations only and should not be used as the sole basis to make medical practice decisions or for disciplinary action against any employee. The statements and recommendations contained in this report are primarily based on the opinions of experts, rather than on scientifically verified data. The ASE makes no express or implied warranties regarding the completeness or accuracy of the information in this report, including the warranty of merchantability or fitness for a particular purpose. In no event shall ASE be liable to you, your patients, or any other third parties for any decision made or action taken by you or such other parties in reliance on this information. Nor does your use of this information constitute the offering of medical advice by the ASE or create any physician-patient relationship between the ASE and your patients or anyone else.

## REFERENCES

- Lang RM, Bierig M, Devereux RB, Flachskampf FA, Foster E, Pellikka PA, et al. Recommendations for chamber quantification: a report from the American Society of Echocardiography's Guidelines and Standards Committee and the Chamber Quantification Writing Group, developed in conjunction with the European Association of Echocardiography, a branch of the European Society of Cardiology. *J Am Soc Echocardiogr* 2005;18:1440-63.
- Forman MB, Goodin J, Phelan B, Kopelman H, Virmani R. Electrocardiographic changes associated with isolated right ventricular infarction. *J Am Coll Cardiol* 1984;4:640-3.
- Kugel MA. Anatomical studies on the coronary arteries and their branches 1 arteria anastomotica auricularis magna. *Am Heart J* 1927;3:260.
- Weyman A. Practices and principles of echocardiography. 2nd ed. Philadelphia: Lippincott, Williams and Wilkins; 1994.
- Otto C. The practice of clinical echocardiography. 3rd ed. Philadelphia: Saunders Elsevier; 2007.
- Gaynor SL, Maniar HS, Prasad SM, Steendijk P, Moon MR. Reservoir and conduit function of right atrium: impact on right ventricular filling and cardiac output. *Am J Physiol Heart Circ Physiol* 2005;288:H2140-5.
- Muller H, Burri H, Lerch R. Evaluation of right atrial size in patients with atrial arrhythmias: comparison of 2D versus real time 3D echocardiography. *Echocardiography* 2008;25:617-23.
- Muller H, Noble S, Keller PF, Sigaud P, Gentil P, Lerch R, et al. Batrial anatomical reverse remodelling after radiofrequency catheter ablation for atrial fibrillation: evidence from real-time three-dimensional echocardiography. *Europace* 2008;10:1073-8.
- Moreno FL, Hagan AD, Holmen JR, Pryor TA, Strickland RD, Castle CH. Evaluation of size and dynamics of the inferior vena cava as an index of right-sided cardiac function. *Am J Cardiol* 1984;53:579-85.
- Brennan JM, Blair JE, Goonewardena S, Ronan A, Shah D, Vasaiwala S, et al. Reappraisal of the use of inferior vena cava for estimating right atrial pressure. *J Am Soc Echocardiogr* 2007;20:857-61.
- Jue J, Chung W, Schiller NB. Does inferior vena cava size predict right atrial pressures in patients receiving mechanical ventilation? *J Am Soc Echocardiogr* 1992;5:613-9.
- Feigenbaum H, Armstrong WF, Ryan T. Feigenbaum's echocardiography. 6th ed. Philadelphia: Lippincott Williams & Wilkins; 2005.
- Weyman A. Cross-sectional echocardiography. Philadelphia: Lea & Febiger; 1981.
- Ommen SR, Nishimura RA, Hurrell DG, Klarich KW. Assessment of right atrial pressure with 2-dimensional and Doppler echocardiography: a simultaneous catheterization and echocardiographic study. *Mayo Clin Proc* 2000;75:24-9.
- Nagueh SF, Kopelen HA, Zoghbi WA. Relation of mean right atrial pressure to echocardiographic and Doppler parameters of right atrial and right ventricular function. *Circulation* 1996;93:1160-9.
- Matsukubo H, Matsuura T, Endo N, Asayama J, Watanabe T. Echocardiographic measurement of right ventricular wall thickness. A new application of subxiphoid echocardiography. *Circulation* 1977;56:278-84.
- Tsuda T, Sawayama T, Kawai N, Katoh T, Nezuo S, Kikawa K. Echocardiographic measurement of right ventricular wall thickness in adults by anterior approach. *Br Heart J* 1980;44:55-61.
- Prakash R, Matsukubo H. Usefulness of echocardiographic right ventricular measurements in estimating right ventricular hypertrophy and right ventricular systolic pressure. *Am J Cardiol* 1983;51:1036-40.
- Gottdiener JS, Gay JA, Maron BJ, Fletcher RD. Increased right ventricular wall thickness in left ventricular pressure overload: echocardiographic determination of hypertrophic response of the "nonstressed" ventricle. *J Am Coll Cardiol* 1985;6:550-5.
- Haddad F, Hunt SA, Rosenthal DN, Murphy DJ. Right ventricular function in cardiovascular disease, part I: anatomy, physiology, aging, and functional assessment of the right ventricle. *Circulation* 2008;117:1436-48.
- Haddad F, Doyle R, Murphy DJ, Hunt SA. Right ventricular function in cardiovascular disease, part II: pathophysiology, clinical importance, and management of right ventricular failure. *Circulation* 2008;117:1717-31.
- Burgess MI, Mogulkoc N, Bright-Thomas RJ, Bishop P, Egan JJ, Ray SG. Comparison of echocardiographic markers of right ventricular function in determining prognosis in chronic pulmonary disease. *J Am Soc Echocardiogr* 2002;15:633-9.
- Quiroz R, Kucher N, Schoepf UJ, Kipfmüller F, Solomon SD, Costello P, et al. Right ventricular enlargement on chest computed tomography: prognostic role in acute pulmonary embolism. *Circulation* 2004;109:2401-4.
- Fremont B, Pacouret G, Jacobi D, Puglisi R, Charbonnier B, de Labriolle A. Prognostic value of echocardiographic right/left ventricular end-diastolic diameter ratio in patients with acute pulmonary embolism: results from a monocenter registry of 1,416 patients. *Chest* 2008;133:358-62.
- Lai WW, Gauvreau K, Rivera ES, Saleeb S, Powell AJ, Geva T. Accuracy of guideline recommendations for two-dimensional quantification of the right ventricle by echocardiography. *Int J Cardiovasc Imaging* 2008;24:691-8.
- Karunanithi MK, Feneley MP. Limitations of unidimensional indexes of right ventricular contractile function in conscious dogs. *J Thorac Cardiovasc Surg* 2000;120:302-12.
- Foale RA, Nihoyannopoulos P, Ribeiro P, McKenna WJ, Oakley CM, Krikler DM, et al. Right ventricular abnormalities in ventricular tachycardia of right ventricular origin: relation to electrophysiological abnormalities. *Br Heart J* 1986;56:45-54.
- Sugishita Y, Watanabe M, Fisher SA. The development of the embryonic outflow tract provides novel insights into cardiac differentiation and remodeling. *Trends Cardiovasc Med* 2004;14:235-41.
- Dell'Italia LJ. The right ventricle: anatomy, physiology, and clinical importance. *Curr Probl Cardiol* 1991;16:653-720.
- Geva T, Powell AJ, Crawford EC, Chung T, Colan SD. Evaluation of regional differences in right ventricular systolic function by acoustic quantification echocardiography and cine magnetic resonance imaging. *Circulation* 1998;98:339-45.

31. Bashore TM. Adult congenital heart disease: right ventricular outflow tract lesions. *Circulation* 2007;115:1933-47.
32. Arya A, Piorkowski C, Sommer P, Gerds-Li JH, Kottkamp H, Hindricks G. Idiopathic outflow tract tachycardias: current perspectives. *Herz* 2007;32:218-25.
33. Yoerger DM, Marcus F, Sherrill D, Calkins H, Towbin JA, Zareba W, et al. Echocardiographic findings in patients meeting task force criteria for arrhythmogenic right ventricular dysplasia: new insights from the multidisciplinary study of right ventricular dysplasia. *J Am Coll Cardiol* 2005;45:860-5.
34. Anwar AM, Soliman O, van den Bosch AE, McGhie JS, Geleijnse ML, ten Cate FJ, et al. Assessment of pulmonary valve and right ventricular outflow tract with real-time three-dimensional echocardiography. *Int J Cardiovasc Imaging* 2007;23:167-75.
35. Anavekar NS, Gerson D, Skali H, Kwong RY, Yucel EK, Solomon SD. Two-dimensional assessment of right ventricular function: an echocardiographic-MRI correlative study. *Echocardiography* 2007;24:452-6.
36. Nass N, McConnell MV, Goldhaber SZ, Chyu S, Solomon SD. Recovery of regional right ventricular function after thrombolysis for pulmonary embolism. *Am J Cardiol* 1999;83:804-6.
37. Zornoff LA, Skali H, Pfeffer MA, St John SM, Rouleau JL, Lamas GA, et al. Right ventricular dysfunction and risk of heart failure and mortality after myocardial infarction. *J Am Coll Cardiol* 2002;39:1450-5.
38. Anavekar NS, Skali H, Bourgoun M, Ghali JK, Kober L, Maggioni AP, et al. Usefulness of right ventricular fractional area change to predict death, heart failure, and stroke following myocardial infarction (from the VALIANT ECHO study). *Am J Cardiol* 2008;101:607-12.
39. Jiang L, Levine RA, Weyman AE. Echocardiographic assessment of right ventricular volume and function. *Echocardiography* 1997;14:189-206.
40. Helbing WA, Bosch HG, Maliepaard C, Rebergen SA, van der Geest RJ, Hansen B, et al. Comparison of echocardiographic methods with magnetic resonance imaging for assessment of right ventricular function in children. *Am J Cardiol* 1995;76:589-94.
41. Starling MR, Crawford MH, Sorensen SG, O'Rourke RA. A new two-dimensional echocardiographic technique for evaluating right ventricular size and performance in patients with obstructive lung disease. *Circulation* 1982;66:612-20.
42. Silverman NH, Hudson S. Evaluation of right ventricular volume and ejection fraction in children by two-dimensional echocardiography. *Pediatr Cardiol* 1983;4:197-203.
43. Gopal AS, Chukwu EO, Iwuchukwu CJ, Katz AS, Toole RS, Schapiro W, et al. Normal values of right ventricular size and function by real-time 3-dimensional echocardiography: comparison with cardiac magnetic resonance imaging. *J Am Soc Echocardiogr* 2007;20:445-55.
44. Watanabe T, Katsume H, Matsukubo H, Furukawa K, Ijichi H. Estimation of right ventricular volume with two dimensional echocardiography. *Am J Cardiol* 1982;49:1946-53.
45. Linker DT, Moritz WE, Pearlman AS. A new three-dimensional echocardiographic method of right ventricular volume measurement: in vitro validation. *J Am Coll Cardiol* 1986;8:101-6.
46. Fei HW, Wang XF, Xie MX, Zhuang L, Chen LX, Yang Y, et al. Validation of real-time three-dimensional echocardiography for quantifying left and right ventricular volumes: an experimental study. *Chin Med J (Engl)* 2004;117:695-9.
47. Schindera ST, Mehwald PS, Sahn DJ, Kecicioglu D. Accuracy of real-time three-dimensional echocardiography for quantifying right ventricular volume: static and pulsatile flow studies in an anatomic in vitro model. *J Ultrasound Med* 2002;21:1069-75.
48. Hoch M, Vasilyev NV, Soriano B, Gauvreau K, Marx GR. Variables influencing the accuracy of right ventricular volume assessment by real-time 3-dimensional echocardiography: an in vitro validation study. *J Am Soc Echocardiogr* 2007;20:456-61.
49. Grison A, Maschietto N, Reffo E, Stellin G, Padalino M, Vida V, et al. Three-dimensional echocardiographic evaluation of right ventricular volume and function in pediatric patients: validation of the technique. *J Am Soc Echocardiogr* 2007;20:921-9.
50. Heusch A, Lawrenz W, Olivier M, Schmidt KG. Transesophageal 3-dimensional versus cross-sectional echocardiographic assessment of the volume of the right ventricle in children with atrial septal defects. *Cardiol Young* 2006;16:135-40.
51. Nesser HJ, Tkalec W, Patel AR, Masani ND, Niel J, Markt B, et al. Quantitation of right ventricular volumes and ejection fraction by three-dimensional echocardiography in patients: comparison with magnetic resonance imaging and radionuclide ventriculography. *Echocardiography* 2006;23:666-80.
52. Horton KD, Meece RW, Hill JC. Assessment of the right ventricle by echocardiography: a primer for cardiac sonographers. *J Am Soc Echocardiogr* 2009;22:776-92.
53. Endo Y, Maddukuri PV, Vieira ML, Pandian NG, Patel AR. Quantification of right ventricular volumes and function by real time three-dimensional echocardiographic longitudinal axial plane method: validation in the clinical setting. *Echocardiography* 2006;23:853-9.
54. Lu X, Nadvoretzkiy V, Bu L, Stolpen A, Ayres N, Pignatelli RH, et al. Accuracy and reproducibility of real-time three-dimensional echocardiography for assessment of right ventricular volumes and ejection fraction in children. *J Am Soc Echocardiogr* 2008;21:84-9.
55. Niemann PS, Pinho L, Balbach T, Galuschky C, Blankenhagen M, Silberbach M, et al. Anatomically oriented right ventricular volume measurements with dynamic three-dimensional echocardiography validated by 3-Tesla magnetic resonance imaging. *J Am Coll Cardiol* 2007;50:1668-76.
56. Papavassiliou DP, Parks WJ, Hopkins KL, Fyfe DA. Three-dimensional echocardiographic measurement of right ventricular volume in children with congenital heart disease validated by magnetic resonance imaging. *J Am Soc Echocardiogr* 1998;11:770-7.
57. Vogel M, Gutberlet M, Dittrich S, Hosten N, Lange PE. Comparison of transthoracic three dimensional echocardiography with magnetic resonance imaging in the assessment of right ventricular volume and mass. *Heart* 1997;78:127-30.
58. Fujimoto S, Mizuno R, Nakagawa Y, Dohi K, Nakano H. Estimation of the right ventricular volume and ejection fraction by transthoracic three-dimensional echocardiography. A validation study using magnetic resonance imaging. *Int J Card Imaging* 1998;14:385-90.
59. Kjaergaard J, Sogaard P, Hassager C. Quantitative echocardiographic analysis of the right ventricle in healthy individuals. *J Am Soc Echocardiogr* 2006;19:1365-72.
60. Jenkins C, Chan J, Bricknell K, Strudwick M, Marwick TH. Reproducibility of right ventricular volumes and ejection fraction using real-time three-dimensional echocardiography: comparison with cardiac MRI. *Chest* 2007;131:1844-51.
61. Leibundgut G, Rohner A, Grize L, Bernheim A, Kessel-Schaefer A, Bremerich J, et al. Dynamic assessment of right ventricular volumes and function by real-time three-dimensional echocardiography: a comparison study with magnetic resonance imaging in 100 adult patients. *J Am Soc Echocardiogr* 2010;23:116-26.
62. van der Zwaan HB, Helbing WA, McGhie JS, Geleijnse ML, Luijnenburg SE, Roos-Hesselink JW, et al. Clinical value of real-time three-dimensional echocardiography for right ventricular quantification in congenital heart disease: validation with cardiac magnetic resonance imaging. *J Am Soc Echocardiogr* 2010;23:134-40.
63. Grewal J, Majdalany D, Syed I, Pellikka P, Warnes CA. Three-dimensional echocardiographic assessment of right ventricular volume and function in adult patients with congenital heart disease: comparison with magnetic resonance imaging. *J Am Soc Echocardiogr* 2010;23:127-33.
64. Tamborini G, Marsan NA, Gripari P, Maffessanti F, Brusoni D, Muratori M, et al. Reference values for right ventricular volumes and ejection fraction with real-time three-dimensional echocardiography: evaluation in a large series of normal subjects. *J Am Soc Echocardiogr* 2010;23:109-15.
65. Lin SS, Reynertson SI, Louie EK, Levitsky S. Right ventricular volume overload results in depression of left ventricular ejection fraction. Implications for the surgical management of tricuspid valve disease. *Circulation* 1994;90:II209-13.

66. Louie EK, Bieniarz T, Moore AM, Levitsky S. Reduced atrial contribution to left ventricular filling in patients with severe tricuspid regurgitation after tricuspid valvulotomy: a Doppler echocardiographic study. *J Am Coll Cardiol* 1990;16:1617-24.
67. Reynertson SI, Kundur R, Mullen GM, Costanzo MR, McKiernan TL, Louie EK. Asymmetry of right ventricular enlargement in response to tricuspid regurgitation. *Circulation* 1999;100:465-7.
68. Ryan T, Petrovic O, Dillon JC, Feigenbaum H, Conley MJ, Armstrong WF. An echocardiographic index for separation of right ventricular volume and pressure overload. *J Am Coll Cardiol* 1985;5:918-27.
69. Louie EK, Rich S, Levitsky S, Brundage BH. Doppler echocardiographic demonstration of the differential effects of right ventricular pressure and volume overload on left ventricular geometry and filling. *J Am Coll Cardiol* 1992;19:84-90.
70. Mori S, Nakatani S, Kanzaki H, Yamagata K, Take Y, Matsuura Y, et al. Patterns of the interventricular septal motion can predict conditions of patients with pulmonary hypertension. *J Am Soc Echocardiogr* 2008;21:386-93.
71. Galie N, Hinderliter AL, Torbicki A, Fourme T, Simonneau G, Pulido T, et al. Effects of the oral endothelin-receptor antagonist bosentan on echocardiographic and doppler measures in patients with pulmonary arterial hypertension. *J Am Coll Cardiol* 2003;41:1380-6.
72. Raymond RJ, Hinderliter AL, Willis PW, Ralph D, Caldwell EJ, Williams W, et al. Echocardiographic predictors of adverse outcomes in primary pulmonary hypertension. *J Am Coll Cardiol* 2002;39:1214-9.
73. Badesch DB, Champion HC, Sanchez MA, Hooper MM, Loyd JE, Manes A, et al. Diagnosis and assessment of pulmonary arterial hypertension. *J Am Coll Cardiol* 2009;54:S55-66.
74. Lam CS, Borlaug BA, Kane GC, Enders FT, Rodeheffer RJ, Redfield MM. Age-associated increases in pulmonary artery systolic pressure in the general population. *Circulation* 2009;119:2663-70.
75. McQuillan BM, Picard MH, Leavitt M, Weyman AE. Clinical correlates and reference intervals for pulmonary artery systolic pressure among echocardiographically normal subjects. *Circulation* 2001;104:2797-802.
76. McLaughlin VV, Archer SL, Badesch DB, Barst RJ, Farber HW, Lindner JR, et al. ACCF/AHA 2009 expert consensus document on pulmonary hypertension: a report of the American College of Cardiology Foundation Task Force on Expert Consensus Documents and the American Heart Association developed in collaboration with the American College of Chest Physicians; American Thoracic Society, Inc.; and the Pulmonary Hypertension Association. *J Am Coll Cardiol* 2009;53:1573-619.
77. Yock PG, Popp RL. Noninvasive estimation of right ventricular systolic pressure by Doppler ultrasound in patients with tricuspid regurgitation. *Circulation* 1984;70:657-62.
78. Currie PJ, Seward JB, Chan KL, Fyfe DA, Hagler DJ, Mair DD, et al. Continuous wave Doppler determination of right ventricular pressure: a simultaneous Doppler-catheterization study in 127 patients. *J Am Coll Cardiol* 1985;6:750-6.
79. Fisher MR, Forfia PR, Chamara E, Houston-Harris T, Champion HC, Girgis RE, et al. Accuracy of Doppler echocardiography in the hemodynamic assessment of pulmonary hypertension. *Am J Respir Crit Care Med* 2009;179:615-21.
80. Hinderliter AL, Willis PW, Barst RJ, Rich S, Rubin LJ, Badesch DB, et al. Primary Pulmonary Hypertension Study Group. Effects of long-term infusion of prostacyclin (epoprostenol) on echocardiographic measures of right ventricular structure and function in primary pulmonary hypertension. *Circulation* 1997;95:1479-86.
81. Mahan G, Dabestani A, Gardin J, Allie A, Burn C, Henry W. Estimation of pulmonary artery pressure by pulsed Doppler echocardiography. *Circulation* 1983;68:367.
82. Dabestani A, Mahan G, Gardin JM, Takenaka K, Burn C, Allie A, et al. Evaluation of pulmonary artery pressure and resistance by pulsed Doppler echocardiography. *Am J Cardiol* 1987;59:662-8.
83. Abbas AE, Fortuin FD, Schiller NB, Appleton CP, Moreno CA, Lester SJ. Echocardiographic determination of mean pulmonary artery pressure. *Am J Cardiol* 2003;92:1373-6.
84. Aduen JF, Castello R, Lozano MM, Hepler GN, Keller CA, Alvarez F, et al. An alternative echocardiographic method to estimate mean pulmonary artery pressure: diagnostic and clinical implications. *J Am Soc Echocardiogr* 2009;22:814-9.
85. Ristow B, Schiller NB. Stepping away from ritual right heart catheterization into the era of noninvasively measured pulmonary artery pressure. *J Am Soc Echocardiogr* 2009;22:820-2.
86. Milan A, Magnino C, Veglio F. Echocardiographic indexes for the non-invasive evaluation of pulmonary hemodynamics. *J Am Soc Echocardiogr* 2010;23:225-39.
87. Abbas AE, Fortuin FD, Schiller NB, Appleton CP, Moreno CA, Lester SJ. A simple method for noninvasive estimation of pulmonary vascular resistance. *J Am Coll Cardiol* 2003;41:1021-7.
88. Farzaneh-Far R, McKeown BH, Dang D, Roberts J, Schiller NB, Foster E. Accuracy of Doppler-estimated pulmonary vascular resistance in patients before liver transplantation. *Am J Cardiol* 2008;101:259-62.
89. Farzaneh-Far R, Na B, Whooley MA, Schiller NB. Usefulness of noninvasive estimate of pulmonary vascular resistance to predict mortality, heart failure, and adverse cardiovascular events in patients with stable coronary artery disease (from the Heart and Soul Study). *Am J Cardiol* 2008;101:762-6.
90. Rajagopalan N, Simon MA, Suffoletto MS, Shah H, Edelman K, Mathier MA, et al. Noninvasive estimation of pulmonary vascular resistance in pulmonary hypertension. *Echocardiography* 2009;26:489-94.
91. Grunig E, Weissmann S, Ehlken N, Fijalkowska A, Fischer C, Fourme T, et al. Stress Doppler echocardiography in relatives of patients with idiopathic and familial pulmonary arterial hypertension: results of a multicenter European analysis of pulmonary artery pressure response to exercise and hypoxia. *Circulation* 2009;119:1747-57.
92. Bossone E, Rubenfire M, Bach DS, Ricciardi M, Armstrong WF. Range of tricuspid regurgitation velocity at rest and during exercise in normal adult men: implications for the diagnosis of pulmonary hypertension. *J Am Coll Cardiol* 1999;33:1662-6.
93. Scapellato F, Temporelli PL, Eleuteri E, Corra U, Imparato A, Giannuzzi P. Accurate noninvasive estimation of pulmonary vascular resistance by Doppler echocardiography in patients with chronic failure heart failure. *J Am Coll Cardiol* 2001;37:1813-9.
94. Dehnert C, Grunig E, Mereles D, von Lennep N, Bartsch P. Identification of individuals susceptible to high-altitude pulmonary oedema at low altitude. *Eur Respir J* 2005;25:545-51.
95. Grunig E, Janssen B, Mereles D, Barth U, Borst MM, Vogt IR, et al. Abnormal pulmonary artery pressure response in asymptomatic carriers of primary pulmonary hypertension gene. *Circulation* 2000;102:1145-50.
96. Bidart CM, Abbas AE, Parish JM, Chaliki HP, Moreno CA, Lester SJ. The noninvasive evaluation of exercise-induced changes in pulmonary artery pressure and pulmonary vascular resistance. *J Am Soc Echocardiogr* 2007;20:270-5.
97. Gleason WL, Braunwald E. Studies on the first derivative of the ventricular pressure pulse in man. *J Clin Invest* 1962;41:80-91.
98. Anconina J, Danchin N, Selton-Suty C, Isaaq K, Juilliere Y, Buffet P, et al. Measurement of right ventricular dP/dt. A simultaneous/comparative hemodynamic and Doppler echocardiographic study [article in French]. *Arch Mal Coeur Vaiss* 1992;85:1317-21.
99. Anconina J, Danchin N, Selton-Suty C, Isaaq K, Juilliere Y, Buffet P, et al. Noninvasive estimation of right ventricular dP/dt in patients with tricuspid valve regurgitation. *Am J Cardiol* 1993;71:1495-7.
100. Tei C, Dujardin KS, Hodge DO, Bailey KR, McGoon MD, Tajik AJ, et al. Doppler echocardiographic index for assessment of global right ventricular function. *J Am Soc Echocardiogr* 1996;9:838-47.
101. Yoshifuku S, Otsuji Y, Takasaki K, Yuge K, Kisanuki A, Toyonaga K, et al. Pseudonormalized Doppler total ejection isovolume (Tei) index in patients with right ventricular acute myocardial infarction. *Am J Cardiol* 2003;91:527-31.
102. Rojo EC, Rodrigo JL, Perez de Isla L, Almeria C, Gonzalo N, Aubele A, et al. Disagreement between tissue Doppler imaging and conventional



- pulsed wave Doppler in the measurement of myocardial performance index. *Eur J Echocardiogr* 2006;7:356-64.
103. Gaibazzi N, Petrucci N, Ziacchi V. Left ventricle myocardial performance index derived either by conventional method or mitral annulus tissue-Doppler: a comparison study in healthy subjects and subjects with heart failure. *J Am Soc Echocardiogr* 2005;18:1270-6.
104. Sebbag I, Rudski LG, Therrien J, Hirsch A, Langleben D. Effect of chronic infusion of epoprostenol on echocardiographic right ventricular myocardial performance index and its relation to clinical outcome in patients with primary pulmonary hypertension. *Am J Cardiol* 2001;88:1060-3.
105. Abd El Rahman MY, Abdul-Khalik H, Vogel M, Alexi-Meskischvili V, Gutberlet M, Hetzer R, et al. Value of the new Doppler-derived myocardial performance index for the evaluation of right and left ventricular function following repair of tetralogy of Fallot. *Pediatr Cardiol* 2002;23:502-7.
106. Chockalingam A, Gnanavelu G, Alagesan R, Subramaniam T. Myocardial performance index in evaluation of acute right ventricular myocardial infarction. *Echocardiography* 2004;21:487-94.
107. Eidem BW, O'Leary PW, Tei C, Seward JB. Usefulness of the myocardial performance index for assessing right ventricular function in congenital heart disease. *Am J Cardiol* 2000;86:654-8.
108. Moller JE, Sondergaard E, Poulsen SH, Appleton CP, Egstrup K. Serial Doppler echocardiographic assessment of left and right ventricular performance after a first myocardial infarction. *J Am Soc Echocardiogr* 2001;14:249-55.
109. Morner S, Lindqvist P, Waldenstrom A, Kazzam E. Right ventricular dysfunction in hypertrophic cardiomyopathy as evidenced by the myocardial performance index. *Int J Cardiol* 2008;124:57-63.
110. Schwertmann M, Samman AM, Salehian O, Holm J, Provost Y, Webb GD, et al. Comparison of echocardiographic and cardiac magnetic resonance imaging for assessing right ventricular function in adults with repaired tetralogy of Fallot. *Am J Cardiol* 2007;99:1593-7.
111. Kaul S, Tei C, Hopkins JM, Shah PM. Assessment of right ventricular function using two-dimensional echocardiography. *Am Heart J* 1984;107:526-31.
112. Lopez-Candales A, Dohi K, Rajagopalan N, Edelman K, Gulyasy B, Bazaz R. Defining normal variables of right ventricular size and function in pulmonary hypertension: an echocardiographic study. *Postgrad Med J* 2008;84:40-5.
113. Miller D, Farah MG, Liner A, Fox K, Schluchter M, Hoit BD. The relation between quantitative right ventricular ejection fraction and indices of tricuspid annular motion and myocardial performance. *J Am Soc Echocardiogr* 2004;17:443-7.
114. Tamborini G, Pepi M, Galli CA, Maltagliati A, Celeste F, Muratori M, et al. Feasibility and accuracy of a routine echocardiographic assessment of right ventricular function. *Int J Cardiol* 2007;115:86-9.
115. Lindqvist P, Waldenstrom A, Henein M, Morner S, Kazzam E. Regional and global right ventricular function in healthy individuals aged 20-90 years: a pulsed Doppler tissue imaging study: Umea General Population Heart Study. *Echocardiography* 2005;22:305-14.
116. Kukulski T, Hubbert L, Arnold M, Wranne B, Hatle L, Sutherland GR. Normal regional right ventricular function and its change with age: a Doppler myocardial imaging study. *J Am Soc Echocardiogr* 2000;13:194-204.
117. Nikitin NP, Witte KK, Thackray SD, de Silva R, Clark AL, Cleland JG. Longitudinal ventricular function: normal values of atrioventricular annular and myocardial velocities measured with quantitative two-dimensional color Doppler tissue imaging. *J Am Soc Echocardiogr* 2003;16:906-21.
118. Duan YY, Harada K, Toyono M, Ishii H, Tamura M, Takada G. Effects of acute preload reduction on myocardial velocity during isovolumic contraction and myocardial acceleration in pediatric patients. *Pediatr Cardiol* 2006;27:32-6.
119. Kjaergaard J, Snyder EM, Hassager C, Oh JK, Johnson BD. Impact of preload and afterload on global and regional right ventricular function and pressure: a quantitative echocardiography study. *J Am Soc Echocardiogr* 2006;19:515-21.
120. Pauliks LB, Chan KC, Chang D, Kirby SK, Logan L, DeGroff CG, et al. Regional myocardial velocities and isovolumic contraction acceleration before and after device closure of atrial septal defects: a color tissue Doppler study. *Am Heart J* 2005;150:294-301.
121. Vogel M, Schmidt MR, Kristiansen SB, Cheung M, White PA, Sorensen K, et al. Validation of myocardial acceleration during isovolumic contraction as a novel noninvasive index of right ventricular contractility: comparison with ventricular pressure-volume relations in an animal model. *Circulation* 2002;105:1693-9.
122. Tousignant CP, Bowry R, Levesque S, Denault AY. Regional differences in color tissue Doppler-derived measures of longitudinal right ventricular function using transesophageal and transthoracic echocardiography. *J Cardiothorac Vasc Anesth* 2008;22:400-5.
123. Tugcu A, Guzel D, Yildirimturk O, Aytekin S. Evaluation of right ventricular systolic and diastolic function in patients with newly diagnosed obstructive sleep apnea syndrome without hypertension. *Cardiology* 2009;113:184-92.
124. Sade LE, Ozin B, Ulus T, Acikel S, Pirat B, Bilgi M, et al. Right ventricular contractile reserve in mitral stenosis: implications on hemodynamic burden and clinical outcome. *Int J Cardiol* 2009;135:193-201.
125. Tayyareci Y, Nisanci Y, Umman B, Oncul A, Yurdakul S, Altun I, et al. Early detection of right ventricular systolic dysfunction by using myocardial acceleration during isovolumic contraction in patients with mitral stenosis. *Eur J Echocardiogr* 2008;9:516-21.
126. Toyono M, Harada K, Tamura M, Yamamoto F, Takada G. Myocardial acceleration during isovolumic contraction as a new index of right ventricular contractile function and its relation to pulmonary regurgitation in patients after repair of tetralogy of Fallot. *J Am Soc Echocardiogr* 2004;17:332-7.
127. Vogel M, Derrick G, White PA, Cullen S, Aichner H, Deanfield J, et al. Systemic ventricular function in patients with transposition of the great arteries after atrial repair: a tissue Doppler and conductance catheter study. *J Am Coll Cardiol* 2004;43:100-6.
128. Vogel M, Vogt M. Noninvasive assessment of right ventricular contractile performance. In: Redington AN, Van Arsdell GS, Anderson RH, editors. *Congenital diseases in the right heart*. London: Springer; 2009. pp. 207-12.
129. Jamal F, Bergerot C, Argaud L, Loufouat J, Ovize M. Longitudinal strain quantitates regional right ventricular contractile function. *Am J Physiol Heart Circ Physiol* 2003;285:H2842-7.
130. Berg S. Myocardial Strain Rate by Doppler Ultrasound Methods. Angle dependency and error estimation. Master's thesis, Department of Engineering Cybernetics, NTNU, Trondheim, Norway 2004.
131. Sutherland GR, Di Salvo G, Claus P, D'hooge J, Bijmens B. Strain and strain rate imaging: a new clinical approach to quantifying regional myocardial function. *J Am Soc Echocardiogr* 2004;17:788-802.
132. Kjaergaard J, Sogaard P, Hassager C. Right ventricular strain in pulmonary embolism by Doppler tissue echocardiography. *J Am Soc Echocardiogr* 2004;17:1210-2.
133. Kittipovanonth M, Bellavia D, Chandrasekaran K, Villarraga HR, Abraham TP, Pelikka PA. Doppler myocardial imaging for early detection of right ventricular dysfunction in patients with pulmonary hypertension. *J Am Soc Echocardiogr* 2008;21:1035-41.
134. Chow PC, Liang XC, Cheung EW, Lam WW, Cheung YF. New two-dimensional global longitudinal strain and strain rate imaging for assessment of systemic right ventricular function. *Heart* 2008;94:855-9.
135. Koyama J, Ray-Sequin PA, Falk RH. Longitudinal myocardial function assessed by tissue velocity, strain, and strain rate tissue Doppler echocardiography in patients with AL (primary) cardiac amyloidosis. *Circulation* 2003;107:2446-52.
136. Lindqvist P, Olofsson BO, Backman C, Suhr O, Waldenstrom A. Pulsed tissue Doppler and strain imaging discloses early signs of infiltrative cardiac disease: a study on patients with familial amyloidotic polyneuropathy. *Eur J Echocardiogr* 2006;7:22-30.
137. Sun JP, Stewart WJ, Yang XS, Donnell RO, Leon AR, Felner JM, et al. Differentiation of hypertrophic cardiomyopathy and cardiac amyloidosis from other causes of ventricular wall thickening by two-dimensional strain imaging echocardiography. *Am J Cardiol* 2009;103:411-5.

138. Fujii J, Yazaki Y, Sawada H, Aizawa T, Watanabe H, Kato K. Noninvasive assessment of left and right ventricular filling in myocardial infarction with a two-dimensional Doppler echocardiographic method. *J Am Coll Cardiol* 1985;5:1155-60.
139. Yanase O, Motomiya T, Tejima T, Nomura S. Doppler echocardiographic assessment of right ventricular filling characteristics in hemodynamically significant right ventricular infarction. *Am J Noninvasiv Cardiol* 1992;6:230-6.
140. Yilmaz M, Erol MK, Acikel M, Sevimli S, Alp N. Pulsed Doppler tissue imaging can help to identify patients with right ventricular infarction. *Heart Vessels* 2003;18:112-6.
141. Berman GO, Reichel N, Brownson D, Douglas PS. Effects of sample volume location, imaging view, heart rate and age on tricuspid velocimetry in normal subjects. *Am J Cardiol* 1990;65:1026-30.
142. Bove AA, Santamore WP. Ventricular interdependence. *Prog Cardiovasc Dis* 1981;23:365-88.
143. Courtois M, Barzilai B, Gutierrez F, Ludbrook PA. Characterization of regional diastolic pressure gradients in the right ventricle. *Circulation* 1990;82:1413-23.
144. Dell'Italia LJ, Walsh RA. Right ventricular diastolic pressure-volume relations and regional dimensions during acute alterations in loading conditions. *Circulation* 1988;77:1276-82.
145. Weber KT, Janicki JS, Shroff S, Fishman AP. Contractile mechanics and interaction of the right and left ventricles. *Am J Cardiol* 1981;47:686-95.
146. Pye MP, Pringle SD, Cobbe SM. Reference values and reproducibility of Doppler echocardiography in the assessment of the tricuspid valve and right ventricular diastolic function in normal subjects. *Am J Cardiol* 1991;67:269-73.
147. Klein AL, Leung DY, Murray RD, Urban LH, Bailey KR, Tajik AJ. Effects of age and physiologic variables on right ventricular filling dynamics in normal subjects. *Am J Cardiol* 1999;84:440-8.
148. Redington AN, Penny D, Rigby ML, Hayes A. Antegrade diastolic pulmonary arterial flow as a marker of right ventricular restriction after complete repair of pulmonary atresia with intact septum and critical pulmonary valvar stenosis. *Cardiol Young* 1992;2:382-6.
149. Innelli P, Esposito R, Olibet M, Nistri S, Galderisi M. The impact of ageing on right ventricular longitudinal function in healthy subjects: a pulsed tissue Doppler study. *Eur J Echocardiogr* 2009;10:491-8.
150. Zoghbi WA, Habib GB, Quinones MA. Doppler assessment of right ventricular filling in a normal population. Comparison with left ventricular filling dynamics. *Circulation* 1990;82:1316-24.
151. Yu CM, Lin H, Ho PC, Yang H. Assessment of left and right ventricular systolic and diastolic synchronicity in normal subjects by tissue Doppler echocardiography and the effects of age and heart rate. *Echocardiography* 2003;20:19-27.
152. Berman JL, Green LH, Grossman W. Right ventricular diastolic pressure in coronary artery disease. *Am J Cardiol* 1979;44:1263-8.
153. Wells DE, Befeler B. Dysfunction of the right ventricle in coronary artery disease. *Chest* 1974;66:230-5.
154. Guazzi M, Maltagliati A, Tamborini G, Celeste F, Pepi M, Muratori M, et al. How the left and right sides of the heart, as well as pulmonary venous drainage, adapt to an increasing degree of head-up tilting in hypertrophic cardiomyopathy: differences from the normal heart. *J Am Coll Cardiol* 2000;36:185-93.
155. O'Sullivan CA, Duncan A, Daly C, Li W, Oldershaw P, Henein MY. Dobutamine stress-induced ischemic right ventricular dysfunction and its relation to cardiac output in patients with three-vessel coronary artery disease with angina-like symptoms. *Am J Cardiol* 2005;96:622-7.
156. Pela G, Regolisti G, Coghi P, Cabassi A, Basile A, Cavatorta A, et al. Effects of the reduction of preload on left and right ventricular myocardial velocities analyzed by Doppler tissue echocardiography in healthy subjects. *Eur J Echocardiogr* 2004;5:262-71.
157. Heywood JT, Grimm J, Hess OM, Jakob M, Kraysenbuhl HP. Right ventricular diastolic function during exercise: effect of ischemia. *J Am Coll Cardiol* 1990;16:611-22.
158. Sade LE, Gulmez O, Eroglu S, Sezgin A, Muderrisoglu H. Noninvasive estimation of right ventricular filling pressure by ratio of early tricuspid inflow to annular diastolic velocity in patients with and without recent cardiac surgery. *J Am Soc Echocardiogr* 2007;20:982-8.
159. Sundereswaran L, Nagueh SF, Vardan S, Middleton KJ, Zoghbi WA, Quinones MA, et al. Estimation of left and right ventricular filling pressures after heart transplantation by tissue Doppler imaging. *Am J Cardiol* 1998;82:352-7.
160. Sallach JA, Tang WHW, Borowski AG, Tong W, Porter T, Martin MG, et al. Right atrial volume index in chronic systolic heart failure and prognosis. *JACC Cardiovasc Imaging* 2009;2:527-34.
161. Dernellis J. Right atrial function in hypertensive patients: effects of antihypertensive therapy. *J Hum Hypertens* 2001;15:463-70.
162. Gan CTJ, Holverda S, Marcus JT, Paulus WJ, Marques KM, Bronzwaer JGF, et al. Right ventricular diastolic dysfunction and the acute effects of sildenafil in pulmonary hypertension patients. *Chest* 2007;132:11-7.
163. Sadler DB, Brown J, Nurse H, Roberts J. Impact of hemodialysis on left and right ventricular Doppler diastolic filling indices. *Am J Med Sci* 1992;304:83-90.
164. Turhan S, Tulunay C, Ozduman Cin M, Gursay A, Kilickap M, Dincer I, et al. Effects of thyroxine therapy on right ventricular systolic and diastolic function in patients with subclinical hypothyroidism: a study by pulsed wave tissue Doppler imaging. *J Clin Endocrinol Metab* 2006;91:3490-3.
165. Cresci SG, Goldstein JA. Hemodynamic manifestations of ischemic right heart dysfunction. *Cathet Cardiovasc Diagn* 1992;27:28-33.
166. McConnell MV, Solomon SD, Rayan ME, Come PC, Goldhaber SZ, Lee RT. Regional right ventricular dysfunction detected by echocardiography in acute pulmonary embolism. *Am J Cardiol* 1996;78:469-73.
167. Scridon T, Scridon C, Skali H, Alvarez A, Goldhaber SZ, Solomon SD. Prognostic significance of troponin elevation and right ventricular enlargement in acute pulmonary embolism. *Am J Cardiol* 2005;96:303-5.
168. Ferlinz J. Right ventricular function in adult cardiovascular disease. *Prog Cardiovasc Dis* 1982;25:225-67.
169. Berger PB, Ruocco NA Jr, Ryan TJ, Jacobs AK, Zaret BL, Wackers FJ, et al. The TIMI Research Group. Frequency and significance of right ventricular dysfunction during inferior wall left ventricular myocardial infarction treated with thrombolytic therapy (results from the Thrombolysis In Myocardial Infarction [TIMI] II trial). *Am J Cardiol* 1993;71:1148-52.
170. Gorcsan J III, Murali S, Counihan PJ, Mandarino WA, Kormos RL. Right ventricular performance and contractile reserve in patients with severe heart failure. Assessment by pressure-area relations and association with outcome. *Circulation* 1996;94:3190-7.
171. Polak JF, Holman BL, Wynne J, Colucci WS. Right ventricular ejection fraction: an indicator of increased mortality in patients with congestive heart failure associated with coronary artery disease. *J Am Coll Cardiol* 1983;2:217-24.
172. Di Salvo TG, Mathier M, Semigran MJ, Dec GW. Preserved right ventricular ejection fraction predicts exercise capacity and survival in advanced heart failure. *J Am Coll Cardiol* 1995;25:1143-53.
173. Skali H, Zornoff LA, Pfeffer MA, Arnold MO, Lamas GA, Moye LA, et al. Prognostic use of echocardiography 1 year after a myocardial infarction. *Am Heart J* 2005;150:743-9.
174. Khush KK, Tasissa G, Butler J, McGlothlin D, De Marco T. ESCAPE Investigators. Effect of pulmonary hypertension on clinical outcomes in advanced heart failure: analysis of the Evaluation Study of Congestive Heart Failure and Pulmonary Artery Catheterization Effectiveness (ESCAPE) database. *Am Heart J* 2009;157:1026-34.
175. Romero-Corral A, Somers VK, Pellikka PA, Olson EJ, Bailey KR, Korinek J, et al. Decreased right and left ventricular myocardial performance in obstructive sleep apnea. *Chest* 2007;132:1863-70.
176. Bhattacharyya S, Toumpanakis C, Burke M, Taylor AM, Caplin ME, Davar J. Features of carcinoid heart disease identified by 2- and 3-dimensional echocardiography and cardiac MRI. *Circ Cardiovasc Imaging* 2010;3:103-11.

177. Callahan JA, Wroblewski EM, Reeder GS, Edwards WD, Seward JB, Tajik AJ. Echocardiographic features of carcinoid heart disease. *Am J Cardiol* 1982;50:762-8.
178. Mittal SR, Goozar RS. Echocardiographic evaluation of right ventricular systolic functions in pure mitral stenosis. *Int J Cardiovasc Imaging* 2001;17:13-8.
179. Schenk P, Globits S, Koller J, Brunner C, Artemiou O, Klepetko W, et al. Accuracy of echocardiographic right ventricular parameters in patients with different end-stage lung diseases prior to lung transplantation. *J Heart Lung Transplant* 2000;19:145-54.
180. Jurcut R, Giusca S, La Gerche A, Vasile S, Ginghina C, Voigt JU. The echocardiographic assessment of the right ventricle: what to do in 2010? *Eur J Echocardiogr* 2010;11:81-96.
181. Shiota T. 3D echocardiography: evaluation of the right ventricle. *Curr Opin Cardiol* 2009;24:410-4.
182. Lytrivi ID, Lai WW, Ko HH, Nielsen JC, Parness IA, Srivastava S. Color Doppler tissue imaging for evaluation of right ventricular systolic function in patients with congenital heart disease. *J Am Soc Echocardiogr* 2005;18:1099-104.